





# Using stable water isotopes to understand ecohydrological partitioning under contrasting land uses in a drought-sensitive rural, lowland catchment

Jessica Landgraf<sup>1,2</sup>  | Dörthe Tetzlaff<sup>1,2,3</sup>  | Songjun Wu<sup>1,2</sup>  |  
Jonas Freymüller<sup>1</sup> | Chris Soulsby<sup>1,3</sup> 

<sup>1</sup>Department of Ecohydrology and Biogeochemistry, Leibniz Institute of Freshwater Ecology and Inland Fisheries, Berlin, Germany

<sup>2</sup>Department of Geography, Humboldt-Universität zu Berlin, Berlin, Germany

<sup>3</sup>Northern Rivers Institute, Kings College, University of Aberdeen, Old Aberdeen, UK

## Correspondence

Jessica Landgraf, Department of Ecohydrology and Biogeochemistry, Leibniz Institute of Freshwater Ecology and Inland Fisheries, Müggelseedamm 310, 12587 Berlin, Germany. Email: [jessica.landgraf@igb-berlin.de](mailto:jessica.landgraf@igb-berlin.de)

## Funding information

Einstein Research Unit Climate and Water under Change; Leverhulme Trust, Grant/Award Number: RPG 2018 375

## Abstract

Vegetation plays an essential role in water partitioning, as it strongly influences evapotranspiration, infiltration and water retention. To analyse the influence of vegetation on water partitioning under innovative land management strategies, we used stable water isotopes as natural tracers to monitor precipitation, soil water and groundwater fluxes over the growing season of 2021 (March–October). We selected eight plot sites with four contrasting land covers and soil types in the drought-sensitive Demnitzer Millcreek Catchment (DMC) in NE Germany. The land use types include forest, grassland, and arable with the latter being subdivided into conventional (e.g., crops) and innovative (e.g., agroforestry) sites. Two weather stations, a flux tower, and in situ soil moisture monitoring complemented our isotopic data with a hydroclimatic context. The year of 2021 had near-normal precipitation totals compared to the prolonged drought of 2018–20. Soil water storage was highest at the agricultural sites, while lowest at the forest, though this reflected both the influence of soil properties (as forests dominated sand soils while crops loam soils) and the greater evapotranspiration from forests. We also estimated soil water ages and found the greatest isotopic variability and fastest turnover of water in the upper soils of arable sites. The forest soil water had the most limited variability in isotopic composition and tended to be older, revealing lower levels of groundwater recharge. Conventional and innovative cropping sites were similar to each other, likely due to the early tree development stage in agroforestry schemes under the latter. Our investigation revealed the forest sites are potentially most vulnerable to limited water availability in the DMC and land use changes in agricultural land lacked major differences in ecohydrological fluxes over the study year. The study further underlines the need for long-term observations of recent adaptive land use changes and drought-sensitive vegetation to improve our understanding and evolve drought resilient land management strategies considering time lags in impacts and non-stationarity.

This is an open access article under the terms of the [Creative Commons Attribution](https://creativecommons.org/licenses/by/4.0/) License, which permits use, distribution and reproduction in any medium, provided the original work is properly cited.

© 2022 The Authors. *Hydrological Processes* published by John Wiley & Sons Ltd.

## KEYWORDS

drought, ecohydrological partitioning, ecohydrology, intermittent streams, land management, land use, soil moisture, stable water isotopes

## 1 | INTRODUCTION

Plants act as an important interface between soil and the atmosphere and partition water from both media in a variety of ways. They affect incoming precipitation by interception of rainfall and redistribution of net rainfall by throughfall and stemflow (Friesen & Van Stan, 2019). Rooting systems have an impact on soil structure, hydraulic conductivity and soil moisture distribution, influencing both infiltration and runoff (Thompson et al., 2010). During root water uptake, plants access and mix water from different subsurface pools before returning it to the atmosphere (Kühnhammer et al., 2020). As different land uses have contrasting effects on water partitioning and demand, land use changes are able to substantially change patterns of evapotranspiration (ET), infiltration, water retention, and the timing and volume of available water in storage (Balist et al., 2022). Increased recognition of the fundamental importance of plants to water partitioning has brought a shift in the scientific focus from an emphasis on blue (groundwater, stream water, and runoff) to blue-green (green: ET, soil water) water fluxes (Falkenmark & Rockström, 2006), and the influence of land use change on water partitioning has become central to many studies (Geris et al., 2015; Hopp et al., 2009; Msigwa et al., 2021; Sprenger et al., 2017).

Assessing the role of vegetation in water partitioning is especially important as climate change, with decreasing precipitation and increasing atmospheric demand for ET, adds challenges to the protection of ecosystems and development of sustainable land use strategies (see Hänsel et al., 2022). For example, the 2018 drought in central and northern Europe caused severe impacts through crop failure and water stress in forests (Brás et al., 2021; Senf & Seidl, 2021; Smith, Tetzlaff, Kleine, et al., 2020b). As droughts tend to effect blue water fluxes more strongly than green water fluxes (see Orth & Destouni, 2018), groundwater levels can take much longer to recover to reduced recharge (Smith et al., 2021; Wunsch et al., 2022). Therefore, an improved understanding of ecohydrological fluxes and water partitioning under different land use in drought-sensitive landscapes is urgently required to understand how to best sustain important anthropogenically (e.g., freshwater, food, fibre, and shelter) and naturally (e.g., forests, wetlands, and streams) relevant ecosystem services (see Foley et al., 2005).

Considering the likely trend of increased frequency and longevity of drought years in Europe (Jacob et al., 2014), long-term investigations are needed to understand the relationship between drought severity and the timescales of cumulative impacts, which may vary for different geographical regions (see Moravec et al., 2021). Further, the effects of land use change on local water cycling are non-stationary and may take several years to decades before showing measurable changes as different vegetation communities take this time to grow and they may differ in their adaptability according to their life stage (Süßel & Brüggemann, 2021). Evolving adaptive strategies for water management and reducing environmental and economic costs takes time (see Tetzlaff et al., 2017).

As shown in several studies (e.g., Goldsmith et al., 2012; Rothfuss et al., 2010; Smith et al., 2021; Tetzlaff et al., 2015), isotopes have great potential for understanding such ecohydrological changes. Stable water isotopes are effective natural tracers to investigate ecohydrological fluxes of a catchment (Soulsby et al., 2011; Tetzlaff et al., 2015). They are especially useful in resolving ET components through evaporative fractionation signals (Sprenger et al., 2017). Over the last decade, isotopes have been used more extensively due to cheaper analyses by cavity ring-down spectroscopy (CRDS) (Rothfuss et al., 2013; Volkman & Weiler, 2014) and even in situ methods, which are now able to trace isotope dynamics in real time, not only in soil water, but also in xylem water (Beyer et al., 2020; Landgraf et al., 2022). Routine, longer-term monitoring of stable isotopes has the potential to allow the ecohydrological consequences of land use change to be quantitatively assessed. This is timely, as in many areas the water footprint of contrasting agricultural and forestry land use strategies is becoming a matter of increasing concern (Balist et al., 2022; Laganière et al., 2022; Neill et al., 2021). Stable water isotopes have already yielded important insights into land use effects on water partitioning, specifically in terms of variations in soil water dynamics and consequent mixing processes. For example, Sprenger et al. (2017) found spatio-temporal variability of soil water isotopic composition and evaporation loss to be lower for heather (*Ericaceae* spp.) shrub vegetation than for Scots pine (*Pinus* spp.) forest in the Scottish Highlands. Another study in Northern Germany situated in a catchment of a groundwater-fed lake found areas forested with beech (*Fagus* spp.) 'used' higher amounts of precipitation due to interception evaporation and transpiration compared to neighbouring grassland sites, halving the levels of groundwater recharge (Douinot et al., 2019).

The region of Brandenburg in NE Germany is one of the driest regions in central Europe and particularly vulnerable to droughts (Ziche et al., 2021). Previous studies in the region—and in particular during the 2018 drought—using monitoring and modelling of stable water isotopes to assess land use effects on water partitioning showed large land use impacts on water partitioning. In particular, forest sites were drier due to higher interception and transpiration losses compared to an adjacent grassland (Kleine et al., 2020). Forest sites, which tended to be found on more freely draining, less retentive sand soils, also had younger soil water and groundwater recharge ages compared to grassland. This reflected both the higher water use of the forest, and the lower soil moisture storage causing a more pronounced annual cycle of water ages (Smith, Tetzlaff, Kleine, et al., 2020b). After the 2018 drought, the lower forest soil water storage was more rapidly replenished, with the resulting storage being younger compared to grassland (>8 months) (Smith, Tetzlaff, Kleine, et al., 2020b). This shows that different land use types can markedly affect the interactions between water fluxes, storage dynamics and ages, and that these can vary in their response to drought and post-drought recovery. However, understanding and quantifying water partitioning due to vegetation and soil

cover at different spatial and temporal scales is complex and further research on effects of different land use/soil type units on water partitioning is required (see Smith et al., 2021).

In our study, the overarching aim was to investigate more fully the effects of different, representative soil and land use units on ecohydrological partitioning in a drought-sensitive agricultural landscape which has climate change trajectories towards warmer and drier conditions. Current policy formulation is encouraging land owners to new land management strategies moving away from traditional crops and forestry towards what may be more climate-resilient approaches (agroforestry, etc.); though the hydrological impacts of such changes are unclear. We investigated soilwater stable isotopes and other hydrological variables to assess the ecohydrological fluxes under four different soil and land use units. These results also serve to provide a benchmark for understanding longer-term land management in terms of drought resilient land use.

Our specific research questions are:

- How does land use affect soil moisture dynamics?
- How does land use affect the temporal dynamics in the isotopic composition of soil water?
- What role does land use play on water partitioning compared to other environmental factors (like hydroclimatic factors driving atmospheric moisture demand)?

Thus, this study sought to increase our understanding of the role of land use on water partitioning as an evidence base for drought resilient land use and management.

## 2 | DATA AND METHODS

Our study focused on the growing season of 2021 (March–October) though for some variables data capture spanned the calendar year January–December 2021. We aggregated all presented data with sub-daily monitoring frequencies into daily values.

### 2.1 | The Demnitzer Millcreek Catchment

The study plots are situated within the Demnitzer Millcreek Catchment (DMC; area of 66 km<sup>2</sup>) in Brandenburg, NE Germany. DMC is a long-term experimental site, which was established to investigate agricultural pollution (Gelbrecht et al., 1998, 2005), and more recently, ecohydrological fluxes at different scales (Kleine et al., 2020; Kleine, Tetzlaff, Smith, Goldhammer, & Soulsby, 2021; Smith, Tetzlaff, Kleine, et al., 2020a, 2020b). The mid-continental climate is characterised by mean annual precipitation of ~548 mm (1990–2020, weather station Müncheberg, Deutscher Wetter Dienst (DWD), 2021) with occasional high intensity events in summer and more frequent low intensity events in winter. Annual potential ET is 650–700 mm a<sup>-1</sup> (Smith, Tetzlaff, Kleine, et al., 2020a). Annual mean temperature is around 9.7°C (1990–2020, DWD, 2021) with an increasing tendency over the last 30 years (1990–1999: 9.2°C; 2011–2020: 10.1°C, DWD, 2021).

The catchment has a NNE-SSW orientation with an average slope of <2% and is part of the North German Plain (NGP). It was formed by the last glaciation 10–15k years BP (Kleine, Tetzlaff, Smith, Goldhammer, & Soulsby, 2021). Its landscape is shaped by a long history of artificial drainage which was particularly intense in the wetlands of the central catchment part (Gelbrecht et al., 2005). The stream network stretches through fluvial and periglacial sediments bounded by basal tills with the upper catchment dominated by unconsolidated ground moraine deposits. There are four major soil types in the catchment; silty brown earths in the North and South; and sandy gleys, peats, and podzols in the centre and south of the catchment.

The catchment is primarily characterised by agricultural land use (>60%) dominating its northern part. The majority of arable land is not irrigated, resulting in precipitation being their sole water input. In the southern area, forestry (35%), as the second major land use, is prevalent. The remaining area is covered by urban settlements or impervious areas (see Figure 1). Thus, in many ways, the DMC is typical of the lowland and mixed land use landscape of the NGP (Smith, Tetzlaff, Kleine, et al., 2020a).

### 2.2 | The plot sites

The eight plot sites chosen in our study represent the main land use types of the catchment with two forest sites (*Forest A* and *B*), one grassland site with two plots (*Grassland West* and *East*) and four agricultural sites; two of these are traditional crops (*Crops* and *Legumes rotation*) and two are agroforestry schemes (*Pasture with shelter belt* and *Syntropic*). In general, the forests occupy sand soils while the grassland, and especially the arable sites, occupy loam soils. Soil texture and physical characteristics of the sites were determined in the field. The catchment and all plot sites are shown in Figure 1 and photos of the study sites are presented in the supplementary material (Figure S1). The forest sites are mainly situated inside mixed deciduous-coniferous forests while the grassland and arable sites are all located in one sub-catchment of the DMC which has the main land use of non-irrigated agricultural land (see Table 1).

*Forest A* is located in the western centre of the catchment and is dominated by mature oak trees (*Quercus robur*) including other species like Scots pine (*Pinus sylvestris*) and red oak (*Quercus rubra*) (Kleine et al., 2020). In contrast, *Forest B* is located further south with old oak trees (*Q. robur*) and young hornbeams (*Carpinus betulus*) as well as Scots pine (*P. sylvestris*). The soil in both locations has a thick humus layer of 5–10 cm on top (*Forest A* has a thicker humus layer than *Forest B*) with a subsoil dominated by silty sand. The sand becomes less silty with increasing depth. A detailed description of the soil texture at *Forest A* and a representative grassland site with similar soils as the arable sites at the DMC is given by Kleine, Tetzlaff, Smith, Dubbert, and Soulsby (2021).

The grassland site includes two plots—*Grassland West* and *East*—and is located in the East of the catchment. The soil is covered mainly by grass and some herbs (e.g., yarrow). From the North, the site is partly sheltered by a small belt of birch (*Betula* spp.) and aspen (*Populus tremula*) but the actual sampling site was not shaded. The soil mainly consists of till with occasional clasts (up to 8 cm diameter)

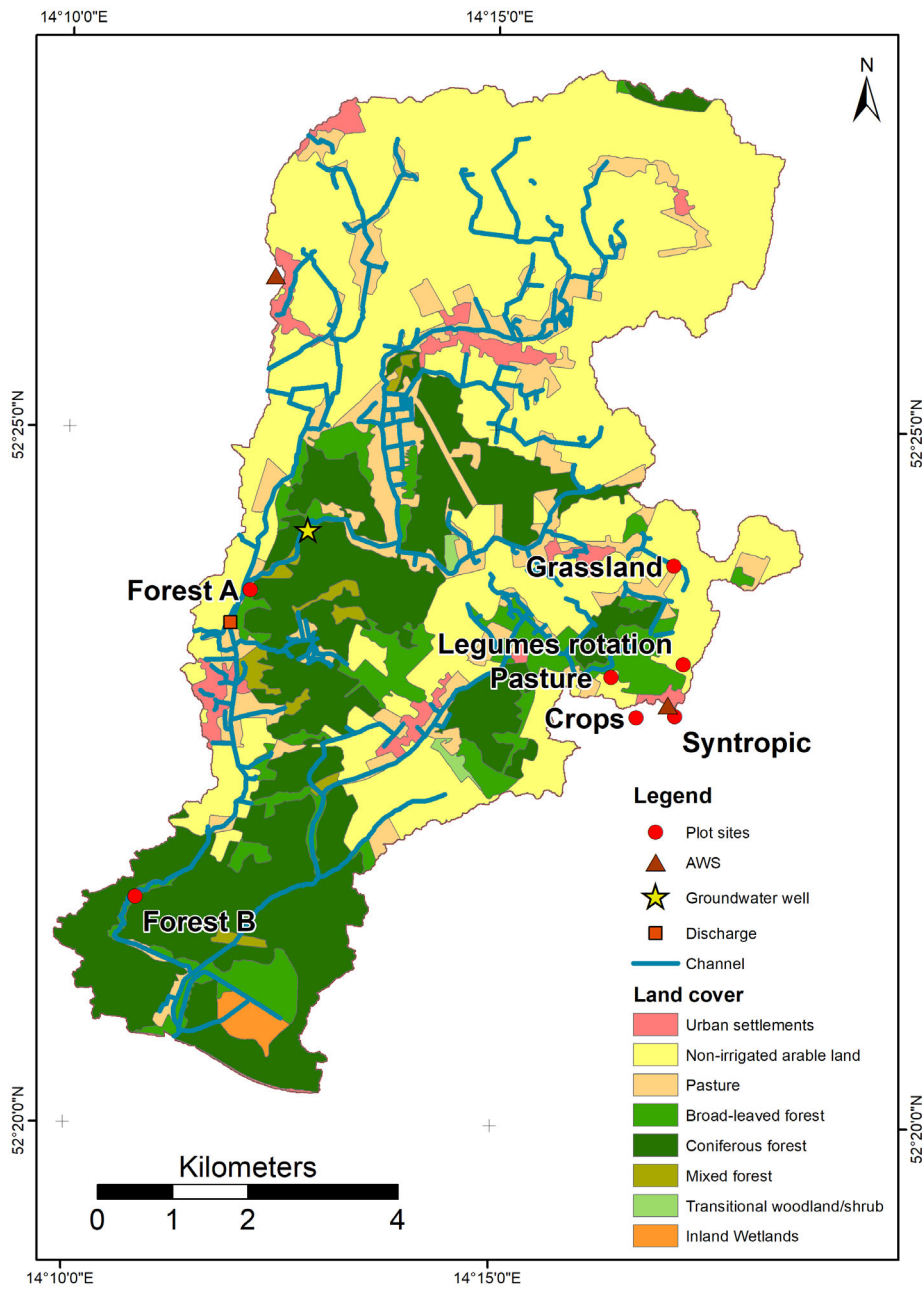


**FIGURE 1** Catchment map showing the location of the plot sites, automatic weather stations and discharge measurement

**TABLE 1** Land use types present in the sub-catchments that contain the different plot sites of this study (GeoBasis-DE / BKG, 2018)

	Area	Urban settlements	Non-irrigated arable land	Pasture	Broad-leaved forest	Coniferous forest	Mixed forest
Name	km <sup>2</sup>	%	%	%	%	%	%
Forest A	4.80	0.1	27.3	7.4	15.3	45.5	4.4
Forest B	6.79	4.9	14.4	8.3	8.0	60.7	3.7
Grassland	8.66	2.6	82.2	14.1	0.0	0.6	0.5
Legumes rotation	8.66	2.6	82.2	14.1	0.0	0.6	0.5
Crops	8.66	2.6	82.2	14.1	0.0	0.6	0.5
Syntropic	8.66	2.6	82.2	14.1	0.0	0.6	0.5
Pasture	8.66	2.6	82.2	14.1	0.0	0.6	0.5

embedded in poorly sorted sand layers. Some small clay lenses can also occur in the layer of 30–50 cm.

The agricultural sites are all located in the East of the catchment—south of *Grassland*—and in close proximity to one another. The sites were covered by different crops representing various agricultural systems, typical for this region. The site *Crops* was covered with rye while the site *Legumes rotation* consisted of a mixture of barley and different herbs. In previous years, cattle has grazed the site but in 2021 no grazing occurred. The two remaining sites represented agroforestry systems. *Pasture with shelter belt* was covered by clover on the pasture part and rows of tree seedlings as well as sun flowers in the belt part. This land use was established quite recently (in winter 2020) and will be developed into a syntropic land use site. The *Syntropic* (combination of small deciduous trees with legumes rotation) plot was covered by clover at its pasture parts with small trees or bushes (up to 2 m in height) arranged in rows roughly 2–3 m apart from one another planted along the site. During the later months of the year, *Syntropic* was partly used as a free range area for chickens. The land use management transforming the site into syntropic agriculture started in 2019. During our monitoring in 2021 numerous mice burrows were observed on site. All the arable sites have similar soil characteristics with brown earth characterising the upper soil (thickness of 10–30 cm), followed by a sandy silt subsoil. At the depth 30–50 cm the material becomes a silty sand.

## 2.3 | Hydroclimatic monitoring

Hydroclimatic conditions were monitored with two automatic weather stations (AWS): one in Hasenfelde (WLV, Environmental Measurement Limited, UK) in the NW of the catchment (since May 2018) and a second one (since May 2019) in the East of the catchment in Alt Madlitz (Campbell Scientific, USA). Both monitored air temperature, precipitation amount, relative humidity, air pressure, wind direction and speed every 15 min. Due to short term power outages, both data sets of air temperature and precipitation amount were merged to provide a continuous data series for the catchment.

Further, an Eddy covariance system (Li-cor Biosciences, Lincoln, NE, USA with LI 7500DS open path analyser; wind measurements via Gill Windmaster pro and a Smart Flux 3 system, frequency 10–20 Hz [Burba, 2013]) was installed in a free standing location at the *Syntropic* site. From March 2021 the system monitored air temperature, precipitation, wind direction and speed, vapour pressure deficit, solar radiation, gas fluxes, and topsoil heat flux as well as moisture at least every 30 min. A detailed overview of the monitoring parameters is presented in Table 2.

## 2.4 | Hydrometric monitoring

We continually monitored volumetric soil water content (VWC) and soil temperature at all sites at an interval of 15 min. The sites *Forest A*, *Grassland* and *Pasture with shelter belt* were equipped with 54 combined soil moisture and temperature probes (SMT-100, Umwelt-

**TABLE 2** Overview of the weather stations, their monitored parameters, interval and measuring days (some data were lost due to power outages)

Station	Parameter	Interval (min)	Days
Hasenfelde	Precipitation	15	292
	Air temperature	15	243
	Relative humidity	15	22
	Wind speed and direction	15	292
Alt Madlitz	Precipitation	15	215
	Air temperature	15	215
	Relative humidity	15	215
	Wind speed and direction	15	215
Eddy covariance	Precipitation	30	266
	Air temperature	30	266
	Wind speed and direction	30	266
	Vapour pressure deficit	30	266
	Solar radiation	30	266
	Gas fluxes	30	201
	Topsoil heat flux	30	201

Geräte-Technik GmbH, Germany). Those sensors measure with frequency domain reflectometry (FDR) utilizing a ring oscillator and resulting in an accuracy of  $\pm 3\%$  for VWC and  $\pm 0.2^\circ\text{C}$  for soil temperature. Each site had two monitored pits (*Forest A South* and *North*, roughly 15 m apart; *Grassland West* and *East*, roughly 400 m apart; *Pasture with shelter belt* one in the pasture and one in a shelter belt, roughly 1 m apart). In *Forest A* and *Grassland*, the pits were segmented into three depths (20, 60, and 100 cm) with two replicas per depth. In *Pasture with shelter belt*, four depths (20, 30, 60, and 100 cm) were monitored with one replica each, except for 20 cm which had two replicas.

At *Forest B*, *Crops*, *Legume rotation*, and *Syntropic*, 30 time domain reflectometry (TDR) probes (CS650, Campbell Scientific, Inc. Logan, UT; accuracy  $\pm 3\%$  for VWC and  $\pm 0.1\%$  for soil temperature) were installed in one pit per site. At *Forest B*, *Crops*, and *Legumes rotation*, the pits were divided into four depths (*Forest B*: 10, 25, 50, and 100 cm; *Crops*: 15, 40, 60, and 100 cm, *Legumes rotation*: 15, 35, 60, 100 cm) with one replica each. *Syntropic* was represented by three depths (20, 40, and 80 cm) with one replica each. A detailed overview on the soil profiles with their according depths and measuring replicas can be found in Tables 3 and 4.

Groundwater level was monitored in a well NNE of *Forest A* close to the southern end of the central wetland (further referred to as GW peat ditch). This well shows seasonal variations that are more generally representative of water table variations throughout the catchment (Kleine, Tetzlaff, Smith, Goldhammer, & Soulsby, 2021). The recording of the water level was conducted by a datalogger (AquiLite ATP 10, AquiTronic Umweltmeßtechnik GmbH, Kirchheim/Teck, Germany) at an interval of 4 h.

Stream water levels (further referred to as Bruch Mill) were monitored south of *Forest A*. The resulting discharge was calculated by



**TABLE 3** Overview of soil moisture sites with the different depths, intervals, and amounts of replicas as well as minimum, median and maximum values of volumetric soil moisture content

Location	Depth	Interval	Replica amount	VWC %		
	cm	min		Minimum	Median	Maximum
Forest A South	20	15	2	5.0	17.0	26.3
	60	15	2	4.5	13.1	20.2
	100	15	2	5.0	9.7	19.1
Forest A North	20	15	2	3.7	15.0	24.1
	60	15	2	4.1	12.5	17.9
	100	15	2	5.9	13.5	22.4
Forest B	10	15	1	0.9	9.2	13.9
	25	15	1	0.6	5.4	9.3
	50	15	1	0.7	4.8	7.6
	100	15	1	1.0	4.3	5.9
Grassland West	20	15	2	4.7	15.4	22.4
	60	15	2	6.1	9.2	10.9
	100	15	2	10.7	16.1	19.3
Grassland East	20	15	2	6.9	18.8	25.1
	60	15	2	11.7	14.0	15.7
	100	15	2	8.7	10.4	12.6
Crops	15	15	1	4.5	20.2	27.9
	40	15	1	8.5	19.5	25.5
	60	15	1	26.8	32.0	35.0
	100	15	1	27.3	33.3	35.2
Legumes rotation	15	15	1	5.8	24.6	29.0
	35	15	1	8.4	23.2	25.8
	60	15	1	22.2	33.3	35.6
	100	15	1	22.4	32.2	33.6
Pasture next to shelter belt	20	15	2	7.7	19.9	27.6
	30	15	1	7.9	17.4	27.3
	60	15	1	10.9	16.4	24.3
	100	15	1	16.5	21.0	26.5
Pasture in shelter belt	20	15	2	6.7	17.3	27.7
	30	15	1	7.8	17.2	27.0
	60	15	1	7.6	11.7	21.7
	100	15	1	6.8	10.0	18.6
Syntropic	20	15	1	5.0	18.9	24.9
	40	15	1	7.1	22.1	25.8
	80	15	1	21.5	30.6	35.6

transferring the water level records (AuiLite ATP 10, AuiTronic Umweltmeßtechnik GmbH, Kirchheim/Teck, Germany) via a rating curve as established by Smith, Tetzlaff, Gelbrecht, et al. (2020).

## 2.5 | Stable water isotope monitoring

For stable water isotope analysis, daily bulk precipitation was sampled using a modified autosampler (ISCO 3700, Teledyne Isco, Lincoln,

USA) equipped with a funnel 1 m above ground level at the Hasenfelde AWS site. Prior to sampling, the bottles of the autosampler were filled with >0.5 cm paraffin oil to prevent evaporation of the sample (cf. International Atomic Energy Agency, 2014). The collected rainfall was sampled below the paraffin surface with a syringe and filtered (0.2 µm, cellulose acetate) in the field.

Bulk soil samples for stable water isotope analyses were collected at all the sites containing topsoil moisture monitoring (*Forest A, Forest B, Grassland West and East, Crops, Legume rotation, Pasture with shelter*

**TABLE 4** Minimum, median and maximum values of isotopic signatures in precipitation, groundwater, stream water, and all bulk soil sampling sites at each depth-segment

Location	Depth in cm	Samples	$\delta^{18}\text{O}$ [VSMOW ‰]			$\delta^2\text{H}$ [VSMOW ‰]		
			Minimum	Median	Maximum	Minimum	Median	Maximum
Precipitation		113	-19.21	-7.09	0.74	-144.89	-50.58	-7.07
Groundwater		9	-8.30	-8.20	-7.96	-57.43	-56.87	-56.19
Surface water		188	-8.84	-8.01	-6.63	-61.17	-55.80	-50.10
Forest A	0-5	10	-10.97	-5.32	-3.33	-84.82	-40.27	-31.38
	5-10	10	-12.04	-6.50	-4.71	-89.83	-47.73	-38.15
	10-20	10	-11.77	-7.41	-5.61	-84.98	-55.44	-45.81
	20-30	10	-11.66	-8.29	-6.59	-83.34	-59.59	-51.15
	30-50	10	-11.70	-9.31	-7.10	-83.09	-73.20	-53.84
Forest B	0-5	10	-10.89	-5.54	-3.09	-85.32	-46.09	-33.23
	5-10	10	-11.48	-6.63	-4.95	-88.15	-52.80	-41.91
	10-20	10	-11.53	-7.72	-6.22	-86.17	-59.71	-49.06
	20-30	10	-11.80	-8.62	-6.78	-86.75	-67.19	-51.00
	30-50	10	-11.60	-9.46	-7.37	-84.31	-72.08	-54.73
Grassland East	0-5	10	-9.78	-4.90	-0.73	-74.89	-40.16	-29.92
	5-10	10	-11.51	-6.62	-4.67	-86.93	-51.45	-37.80
	10-20	10	-12.75	-8.29	-6.21	-93.51	-60.19	-46.90
	20-30	10	-12.79	-9.02	-6.53	-93.56	-66.06	-48.67
	30-50	10	-12.41	-9.30	-6.69	-89.81	-66.84	-50.07
Grassland West	0-5	10	-9.55	-5.39	-1.47	-79.99	-42.15	-24.46
	5-10	10	-11.68	-7.13	-3.44	-87.52	-51.90	-31.13
	10-20	10	-12.82	-8.25	-4.94	-94.17	-61.81	-40.32
	20-30	10	-12.83	-9.48	-6.12	-92.39	-67.70	-44.97
	30-50	10	-11.64	-9.26	-6.34	-82.13	-65.30	-46.51
Crops	0-5	10	-8.12	-4.93	-0.99	-65.18	-37.29	-24.18
	5-10	10	-11.21	-6.92	-4.38	-86.26	-51.69	-36.87
	10-20	10	-11.42	-8.94	-6.42	-82.70	-61.59	-50.09
	20-30	10	-13.75	-9.42	-6.30	-98.71	-63.62	-49.74
	30-50	10	-13.76	-9.25	-6.93	-97.27	-64.13	-49.74
Legumes rotation	0-5	10	-8.99	-5.76	-0.48	-71.75	-46.72	-28.19
	5-10	10	-11.75	-6.68	-4.44	-88.97	-53.37	-33.95
	10-20	10	-11.95	-8.56	-6.08	-85.95	-66.41	-42.86
	20-30	10	-13.13	-9.20	-7.26	-91.39	-68.83	-49.84
	30-50	10	-11.52	-9.41	-7.63	-80.15	-68.09	-52.92
Pasture next to shelter belt	0-5	10	-10.69	-4.90	-1.92	-81.87	-38.04	-28.52
	5-10	10	-12.55	-6.97	-3.83	-95.48	-51.36	-37.97
	10-20	10	-12.31	-7.87	-6.65	-91.45	-59.51	-47.79
	20-30	10	-12.65	-8.19	-7.06	-92.96	-60.15	-46.73
	30-50	10	-11.16	-9.16	-7.72	-82.02	-65.32	-60.54
Syntropic	0-5	10	-10.37	-5.75	-0.10	-79.82	-44.89	-24.93
	5-10	10	-11.99	-7.39	-2.96	-91.02	-55.16	-36.77
	10-20	10	-12.91	-8.62	-6.56	-95.85	-64.45	-49.52
	20-30	10	-14.59	-9.64	-7.58	-102.97	-68.39	-55.27
	30-50	10	-12.29	-9.73	-8.20	-93.97	-68.19	-61.36

belt, *Syntropic*) on a triweekly-monthly basis (March–October, and one additional sampling in December 2021). Each location was sampled at five depths (0–5, 5–10, 10–20, 20–30, and 30–50 cm) with two replicas per depth. The soil was collected using a core cutter (diameter: 8 cm) for the first two depths (0–5 and 5–10 cm) and afterwards the sampling continued with a hand auger (diameter: 3 cm). For the drier soils at *Forest A* and *B*, a larger auger (diameter: 8 cm) was used to ensure sufficient water amount in the sample since May. Since *Grassland* contained clasts in its till sediments, sampling was conducted via opening trenches and sampling directly from the soil profile using a small shovel since June. The sampled soil was quickly stored in metalized bags (CB400-420siZ, WEBER Packaging GmbH, Güglingen, Germany) and zip locked airtight. Similar to the direct-equilibrium method (cf. Wassenaar et al., 2008) the headspace of the bags was filled with artificial air and equilibrated for roughly 48 h. Next, the headspace of each bag was sampled by carefully piercing the bags with a cannula attached to an off-axis integrated cavity output spectroscopy (OA-ICOS) triple water vapour isotope analyser (TWIA-45-EP, Los Gatos Research, Inc., San Jose, CA). Each bag was measured for roughly 8 min to ensure a stable plateau and thus, reliable data. The same procedure was conducted with standard samples containing 10 ml of water (known isotopic composition), except for measuring for 10 min due to a larger headspace. From those measurements, curve fitting was used to identify the plateau and exclude the beginning of the measurement before a stable plateau was reached. Every 5–6 samples, a standard was measured to ensure covering the daily drift of the isotope analyser. After the measurement, the standards ( $\delta^{18}\text{O}$ :  $-10.11\text{‰}$ ,  $-7.68\text{‰}$ ,  $1.53\text{‰}$ ;  $\delta^2\text{H}$ :  $-72.04\text{‰}$ ,  $-56.70\text{‰}$ ,  $16.74\text{‰}$ ) were used to convert the soil vapour into liquid phase results. All isotopic results given (precipitation, groundwater, stream, soil water, and standards) are relative to the Vienna Standard Mean Ocean Water (VSMOW).

Further, stable water isotopes were monitored in GW peat ditch by monthly sampling. At least twice the volume of water filling the well was pumped with a small groundwater pump (COMET-Pumpen Systemtechnik GmbH & Co. KG, Pfaffschwende, Germany) before sampling with a syringe and filtering (0.2  $\mu\text{m}$ , cellulose acetate) the sample in the field.

Stream stable water isotopes were sampled daily at Bruch Mill using an autosampler (ISCO 3700, Teledyne Isco, Lincoln, USA). As for the precipitation samples, the bottles were filled with a layer of paraffin oil and samples were taken using a syringe and filtered (0.2  $\mu\text{m}$ , cellulose acetate) in the field.

All liquid isotope samples (precipitation, groundwater, and stream) were stored at low temperatures (8°C) until analysed in the laboratory via CRDS (Picarro L2130-i, Picarro Inc., Santa Clara, CA).

## 2.6 | Data analysis

We estimated potential evapotranspiration (PET) via the Penman-Monteith equation (Monteith, 1965; Penman, 1948) implemented in

the FAO Penman-Monteith equation of python (ETo package). The calculation uses the following equation (cf. Allen et al., 1998):

$$ET_0 = \frac{0.408\Delta(R_n - G) + \gamma \frac{900}{T + 273} u_2 (e_s - e_a)}{\Delta + \gamma(1 + 0.34u_2)}, \quad (1)$$

where,  $ET_0$  is the reference evapotranspiration ( $\text{mm day}^{-1}$ ),  $R_n$  is net radiation at the crop surface ( $\text{MJ m}^{-2} \text{day}^{-1}$ ),  $G$  is soil heat flux density ( $\text{MJ m}^{-2} \text{day}^{-1}$ ),  $T$  is mean daily air temperature at 2 m height ( $^{\circ}\text{C}$ ),  $u_2$  is wind speed at 2 m height ( $\text{m s}^{-1}$ ),  $e_s$  is saturation vapour pressure (kPa),  $e_a$  is actual vapour pressure (kPa),  $e_s - e_a$  is saturation vapour pressure deficit (kPa),  $\Delta$  is slope vapour pressure curve ( $\text{kPa } ^{\circ}\text{C}^{-1}$ ),  $\gamma$  is psychrometric constant ( $\text{kPa } ^{\circ}\text{C}^{-1}$ ) with altitude = 98 m, latitude = 52.517588° N, and albedo = 0.23. For further information on the calculation, please check Allen et al. (1998). Our focus was on PET dynamics, hence absolute values may vary depending on aerodynamic and roughness parameters of different vegetation covers.

Soil moisture replicas were averaged (by calculating the mean) over time and depths to gain one daily result for each depth per site.

Soil water storage ( $S$ ) quantifies the amount of water present in a soil volume at a certain point in time. For this, the soil profile was divided into depth-segments representing the different VWC measurements. Soil water storage was calculated via (cf. Maurice, 2013):

$$S = L \cdot \sum_{i=1}^n \theta_i \Delta z_i, \quad (2)$$

where,  $S$  is the soil water storage,  $L$  the depth of the soil profile,  $n$  the number of soil moisture measurements along the profile,  $\theta$  the measured soil moisture, and  $\Delta z$  the depth-segment represented by the according soil moisture measurement. The subdividing of depth-segments depended on the distribution of the different soil moisture probes installed. Soil water storage was estimated according to Equation (2) with  $L$  being 1000 mm for all sites.

Evaporative effects were evaluated using isotope data by calculating the line-conditioned excess (short lc-excess) (cf. Landwehr & Coplen, 2006). The lc-excess describes the deviation from the local meteoric water line (LMWL):

$$\text{lc-excess} = \delta^2\text{H} - a \cdot \delta^{18}\text{O} - b, \quad (3)$$

where,  $a$  is the slope and  $b$  the intercept of the weighted isotopic composition of the local precipitation (for DMC in 2021:  $a = 7.71$ ,  $b = 8.39$ ). Those variables were calculated after Hughes and Crawford (2012) from precipitation amount and isotopic signature from January to December 2021.

We also conducted correlation analyses to identify potential controls on evaporation by evaluating the effect of antecedent conditions (Sprenger et al., 2017). Average values of antecedent PET and sum of precipitation amount as well as weighted isotopic signals over the 7 and 30 days prior to sampling ( $PET_7$ ,  $PET_{30}$ ,  $P_7$ , and  $P_{30}$ ) were calculated.



The statistical analyses of the soil stable water isotopic composition ( $\delta^2\text{H}$ ,  $\delta^{18}\text{O}$ , and Ic-excess) were conducted via the R language and environment for each individual plot site, for all depths and sampling dates. After evaluating the non-normal distribution of some of the data via Shapiro-Wilk test for normality, we continued with non-parametric tests. Differences between the sites ( $n = 1336$ ), sampling dates ( $n = 314$ ), and depths ( $n = 314$ ) were tested by the Kruskal-Wallis test, followed by a post hoc Dunn test ( $p$  value adjustment using a 'Bonferroni' correction) to identify significantly different sampling depths or dates.

Further, mean values of the sampling dates soil water  $\delta^2\text{H}$ ,  $\delta^{18}\text{O}$ , and Ic-excess were tested with  $P_7$ ,  $P_{30}$  and  $PET_7$ ,  $PET_{30}$  for normality by a Shapiro-Wilk test. After confirming that the data were normally distributed, we conducted the  $t$ -test for the mean values of each normally distributed sample group of soil water Ic-excess. Next, we calculated the Pearson correlation coefficients ( $r$ ) describing the linear relationship of two values for those normally distributed sets. Kernel densities were also calculated to visualize the distribution of the stable water isotopes for the different land use types and depths.

The contribution of young water fraction (YWF) to the soil water in each depth was estimated after Kirchner (2016a, 2016b). This method is a simple approach to quantify the contribution of water less than ~2 months old to a stream. Using it for soil water instead of stream water is a coarse, but still useful, method to investigate dynamics rather than comparing absolute values (von Freyberg et al., 2018). In interpreting results, the potential effects of evaporative fraction on soil water isotopes needs to be borne in mind (Marx et al., 2022).

## 3 | RESULTS

### 3.1 | Dynamics in hydroclimate and hydrometrics

With an annual rainfall of ~545 mm and a mean annual temperature of ~9.5°C the hydroclimatic conditions in 2021 were similar to the long-term mean annual characteristics observed by the DWD (precipitation ~548 mm and temperature ~9.7°C; DWD, 2021). There was a large precipitation event on June 30th with roughly 60 mm in 1 day and further six events with precipitation amounts >10 mm out of 134 precipitation events in total in 2021 (only events >0.2 mm were taken into account) (Figure 2a).

However, annual PET (in 2021) of >800 mm surpassed the PET estimated by Smith, Tetzlaff, Gelbrecht, et al. (2020) of 650–700 mm  $\text{a}^{-1}$ . The ET measured by the eddy covariance system maximized to ~10 mm per day, while calculated PET was with ~8 mm per day highest in summer (Figure 2c). Both actual ET and PET showed similar dynamics.

Soil water storage began to decline around May before responding to larger precipitation events during summer. In December 2021, all sites showed lower soil water storages than at the beginning of the year. Soil storage was consistently lowest in *Forest B*. Comparing the

different plot sites, soil moisture was lowest at the forest sites and tended to be wetter in the humus-rich surface horizons (Figures S2 and S3). The arable land use plots had the highest total VWC with a tendency of higher wetness in the subsoil (Figures S2 and S3, see Tables 3 and 4). The relatively recently established innovative arable (agroforestry) sites (*Pasture* and *Syntropic*) were not substantially different in VWC from the conventional sites (*Crops* and *Legumes rotation*). All arable sites (except for *Pasture*) showed less dynamic soil moisture in deeper soil layers (around 60–100 cm) (Figures S2 and S3).

Groundwater levels showed a dominance of winter recharge, peaking in spring and then falling to their lowest level in November. They showed only limited responses to summer precipitation events including the large June event. The stream, which is mainly groundwater-fed, seasonally tracked groundwater variations. The stream system fell dry in July, before beginning to flow again in November as the catchment re-wetted in winter (see Figure 2d–f).

### 3.2 | Dynamics in stable water isotopes

Stable water isotopes in precipitation showed highest, and groundwater the lowest variability (Tables 3 and 4). Precipitation isotope ratios followed the expected seasonality, being most depleted in winter and most enriched in summer, however, day-to-day variability could be high. Soil water isotopic compositions ranged from  $-14.6\text{‰}$  (*Syntropic* 20–30 cm) to  $-0.1\text{‰}$  (*Syntropic* 0–5 cm) for  $\delta^{18}\text{O}$ ; and  $-103\text{‰}$  (*Syntropic* 20–30 cm) to  $-24\text{‰}$  (*Crops* 0–5 cm) for  $\delta^2\text{H}$  (Tables 3 and 4). In general, the soil water isotopic composition was most variable in the upper horizons and then more damped with increasing depth. The Shapiro-Wilk test showed no evidence for data being non-normally distributed (neither site nor depth nor date related).

In the dual isotope plot (Figure 3), all soil water monitoring sites are generally superimposed without any substantial, consistent differences. However, the isotopic compositions of deeper soil horizons were more depleted and damped in their response to precipitation inputs and evaporation effects compared to the upper horizons. Some isotopic results plot below the LMWL (usually from the upper soil horizons in summer), but most clustered in close proximity to it. The *Syntropic* site showed the widest deviation from, while *Forest A* was most similar to the LMWL.

#### 3.2.1 | Seasonal variability

The first part of the study period from March to April showed generally depleted isotopic signals in soil water at all profile depths and all sites (Figures 4 and 5). This was most likely linked to the above-mentioned seasonality in precipitation signals, but also the effects of substantial snowfall (~40 mm rainfall equivalent) and melt in February (see also Figure S5). As summer progressed, isotope ratios for  $\delta^2\text{H}$  and  $\delta^{18}\text{O}$  in soil waters enriched, particularly in the upper soil horizons. However, this enrichment was punctuated by samples with

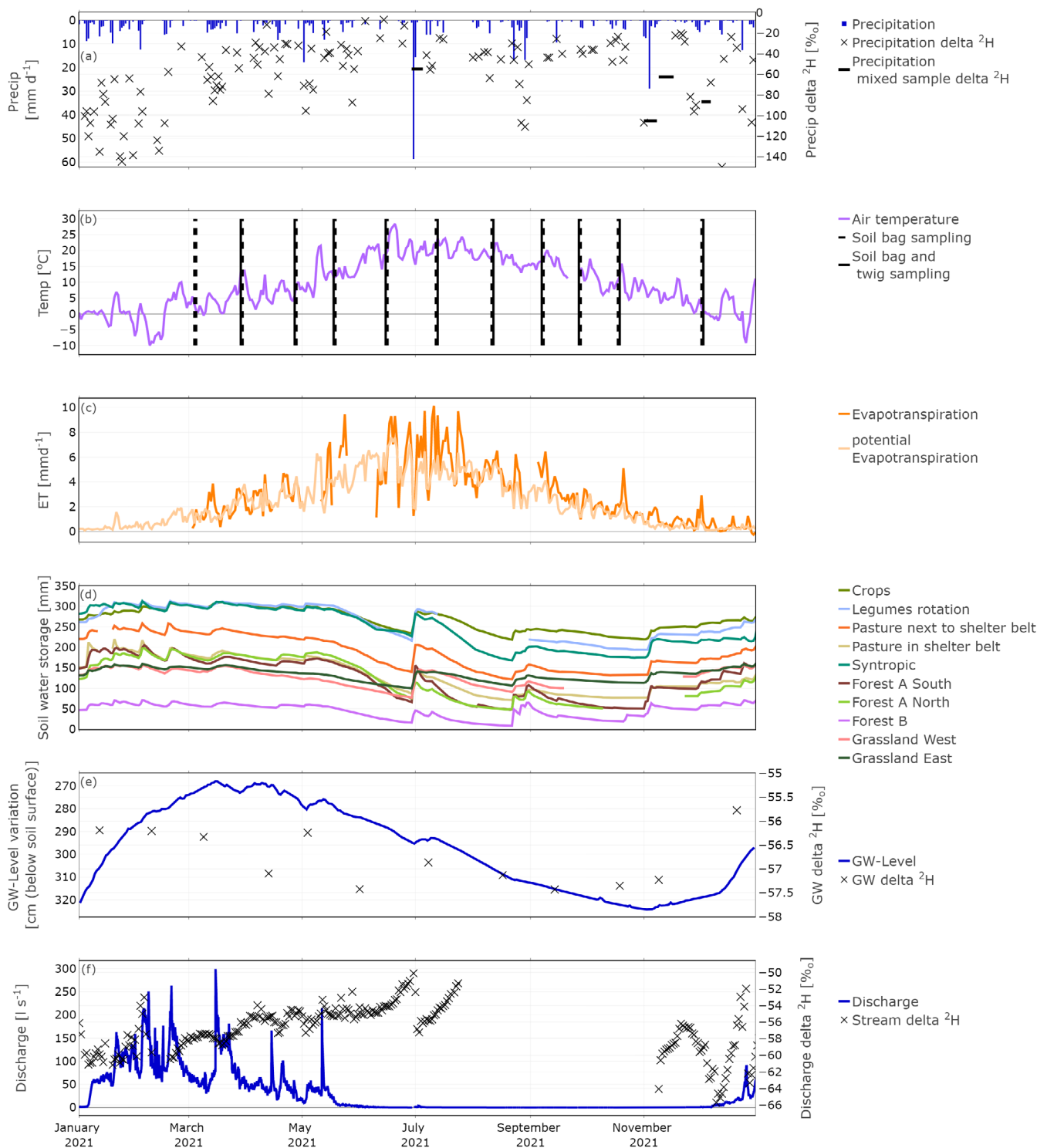


**FIGURE 2** Time series of precipitation daily amount and  $\delta^2\text{H}$  (a), air temperature showing the dates of sampling (b), soil ET (c), soil water storage (d), daily groundwater-level and monthly groundwater  $\delta^2\text{H}$  (e), and discharge (interval 15 min) and  $\delta^2\text{H}$  at Bruch Mill (data gap  $\Rightarrow$  stream fell dry) (f). For presentation purposes, we only show the time series of  $\delta^2\text{H}$  here

more markedly depleted values (e.g., in early September), again most obviously in the upper profile, before a more general depletion of isotope ratios by the end of the year.

Very early on in the year,  $\text{Ic}$ -excess was already depleted (being negative at many sites)—which would be consistent with a memory-effect of the evaporative fractionation during the previous year.

Variability between dates (Figure S5) was linked to precipitation events between each sampling. In June and August, the  $\text{Ic}$ -excess was most depleted, consistent with high evaporative fractionation in the upper soil profile. In some summer samples, the evaporative fractionation had penetrated to depth via percolation in the profile at some of the sites (e.g., *Legumes*).

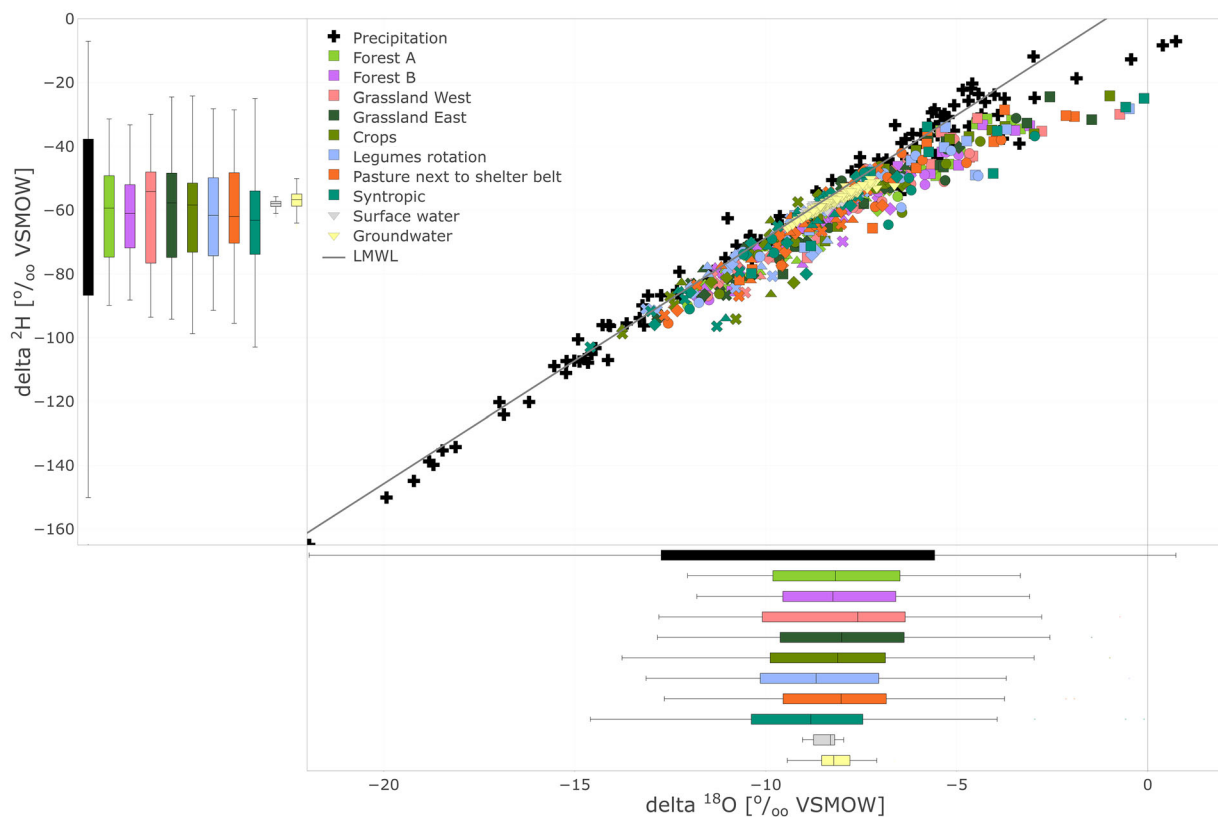


**FIGURE 3** Dual isotope plot showing all data with boxplots representing range and mean values in the data

### 3.2.2 | Spatial variability

In spring, the *Crops*, *Syntropic*, and *Grassland* sites' isotopic composition was enriched in the topsoil (0–10 cm) and depleted below (Figures 4 and 5). This changed in July as more enriched values were also shown for deeper soil layers with a rapid enrichment of all deeper depths (10–20, 20–30, and 30–50 cm). *Legumes* did follow this pattern, but the depleted isotopic signals in spring were less intense. The rapid enrichment in July had similar isotopic compositions ( $-49.1\%$  to  $-54.9\%$   $\delta^2\text{H}$ ,  $-6.2\%$  to  $-8.0\%$   $\delta^{18}\text{O}$  mean over all depths) as the large precipitation event at the end of June. *Pasture* showed depleted isotopic compositions in the topsoil at the first March sampling followed by more enriched results at the end of March which the highest enrichment at the topsoil (0–5 cm). In April and May, enriched and depleted values were found in the topsoil (0–10 cm) and deeper soil layers, respectively. As for the previous sites, all isotope compositions enriched in June, but in general the shift in isotopic composition was less intense as at the other sites. At the *Forest* sites, the deeper soil water isotopes enriched earlier in the year and more gradually, so first 20–30 cm (April), then 30–40 cm (June), and later 40–50 cm (August).

Lc-excess showed no clear spatial patterns being depleted in deeper soil layers (30–50 cm) in *Crops*, *Syntropic*, and *Legumes* in April. The *Grassland* sites showed more enriched lc-excess down to the deep soil (30–50 cm) in April. Both, *Forest* and *Grassland* showed a depletion of lc-excess in May over all depths. Afterwards, there were depletions of lc-excess in the topsoil (0–10 cm) at *Legumes*, *Pasture*, *Syntropic*, and the *Grassland* sites in June and at all sites to various extent in

August. Considering stable water isotopes and lc-excess together the *Forest* sites showed clearly different dynamics from the other sites while differences between *Grassland* and arable sites were minor.

The Kernel density of lc-excess (Figure 6) showed weak variability between sites in terms of land use, which is consistent with the dual isotope plots (Figures 3 and 4). Furthermore, there was weak variability between different depths. Lc-excess was much more variable in the upper horizons than below 10 cm (Figure S6). According to the *post hoc* Dunn test, significant differences for the sites only occasionally occurred in 10–20 and 20–30 cm, with no consistent patterns apparent (Figure S5).

In terms of the YWF, the fitted sine wave for the topsoil (0–5 cm) showed the least attenuation compared to precipitation inputs (Figure 7) reflecting high YWFs of  $>50\%$ . This showed again a strong response in the upper soils at all sites to summer precipitation events, as well as potential fractionation effects from soil evaporation. With increasing depth in the subsoil, the proportion of YWF was generally lower (usually  $<50\%$  at 30–50 cm). In general, the fitted curves showed an attenuation with depths, consistent with advection-dispersion as precipitation mixed with resident soil water and percolated to depth over time (Figure 7) as shown qualitatively in Figures 4 and 5. This was most clear in the forest sites, where the YWF also tended to be lower. The lag-time of the forest sites was shortest (46 days from 5 to 50 cm by  $\delta^2\text{H}$ ) while *Legumes rotation* showed the longest lag-time of 114 days. This is probably linked to soil properties as the water in sandier soils of the forest sites percolated relatively fast. Still, the relatively low lag-time of the forest combined with low

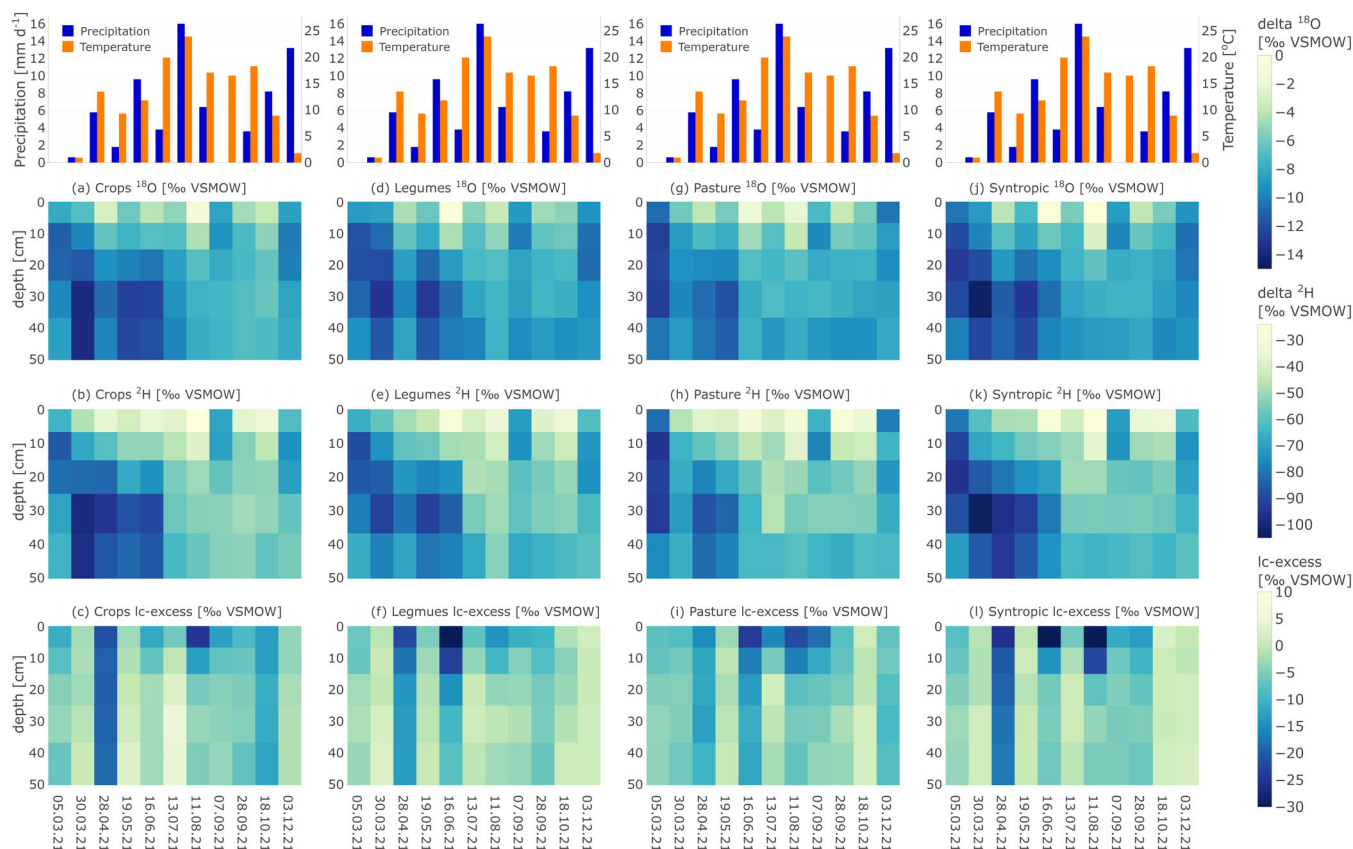


**FIGURE 4** Heat maps of bulk isotopes for *Crops* (a–c), *Legumes rotation* (d–f), *Pasture next to shelter belt* (g–i), and *Syntropic* (j–l). Top histograms show precipitation sum over the previous 7 days and air temperature on the sampling date

YWF indicates that only a small fraction of incoming precipitation percolated to deeper soil layers re-wetting the forest soils. At the other sites, the patterns of YWF were less simple, and more clearly showed the effects of the large rainfall event on 30th of June. The event impacted deeper soil water at most sites (Figures S2 and S3) resulting in relatively high rates of soil water turnover in the study period and high YWFs overall.

### 3.3 | Controls on evaporation

The Pearson correlation coefficient between antecedent precipitation characteristics (30 d, 7 d), PET (30 d, 7 d, and sampling day), air temperature (7 d), and soil water isotopes were combined for all sites and depths (Figure 8). These revealed a moderately strong positive correlation between both soil  $\delta^2\text{H}$  and  $\delta^{18}\text{O}$  at 5 cm depth and PET (0.67 or 0.76 PET<sub>30d</sub>,  $p$ -values <0.05). In contrast, only a weak negative correlation with antecedent precipitation composition ( $-0.32$  Precipitation<sub>7d</sub>  $\delta^2\text{H}$  and  $-0.15$  Precipitation<sub>7d</sub>  $\delta^{18}\text{O}$ ,  $p$ -values >0.05) existed. Soil  $\delta^2\text{H}$  and  $\delta^{18}\text{O}$  at 50 cm correlated negatively to antecedent precipitation ( $-0.63$  or  $-0.57$  Precipitation<sub>30d</sub>  $\delta^2\text{H}$ ,  $p$ -values <0.05) and showed only weak correlation to PET (0.21 or 0.08 PET<sub>30d</sub>,  $p$ -values >0.05). This suggests that the topsoil water isotope composition was more strongly controlled by evaporation effects rather than precipitation. In contrast, PET had limited influence on the isotopic composition of

deeper soil water, which was more strongly influenced by antecedent precipitation, though this was out of phase and lagged by a period indicated by the YWF results. Further, a strong influence of Temperature<sub>7d</sub> on PET<sub>30d</sub> (0.95,  $p$ -value <0.05) was observed.

The soil isotopic composition of the different sampling dates (i.e., all sites combined) showed that summer and autumn  $\delta^2\text{H}$  was most enriched even though PET was much lower in autumn. The conditions of autumn with enriched  $\delta^2\text{H}$  and low PET suggest a cumulative memory effect of influences through the summer on soil water composition (Figure 9a). Lc-excess showed a hysteresis loop with enriched Lc-excess results in winter and depleted values in summer and spring (Figure 9b). However, the loop was less pronounced compared to other studies (see Sprenger et al., 2017) and punctuated by precipitation events, especially the one at the end of June. The large precipitation event reset the Lc-excess to a higher level in July, more comparable to that of precipitation.

## 4 | DISCUSSION

### 4.1 | Effects of land use on soil moisture

The main novelty of this study stems from water stable isotope sampling on a monthly basis over an entire growing period under different several soil/land use types, incl alternative land management types.

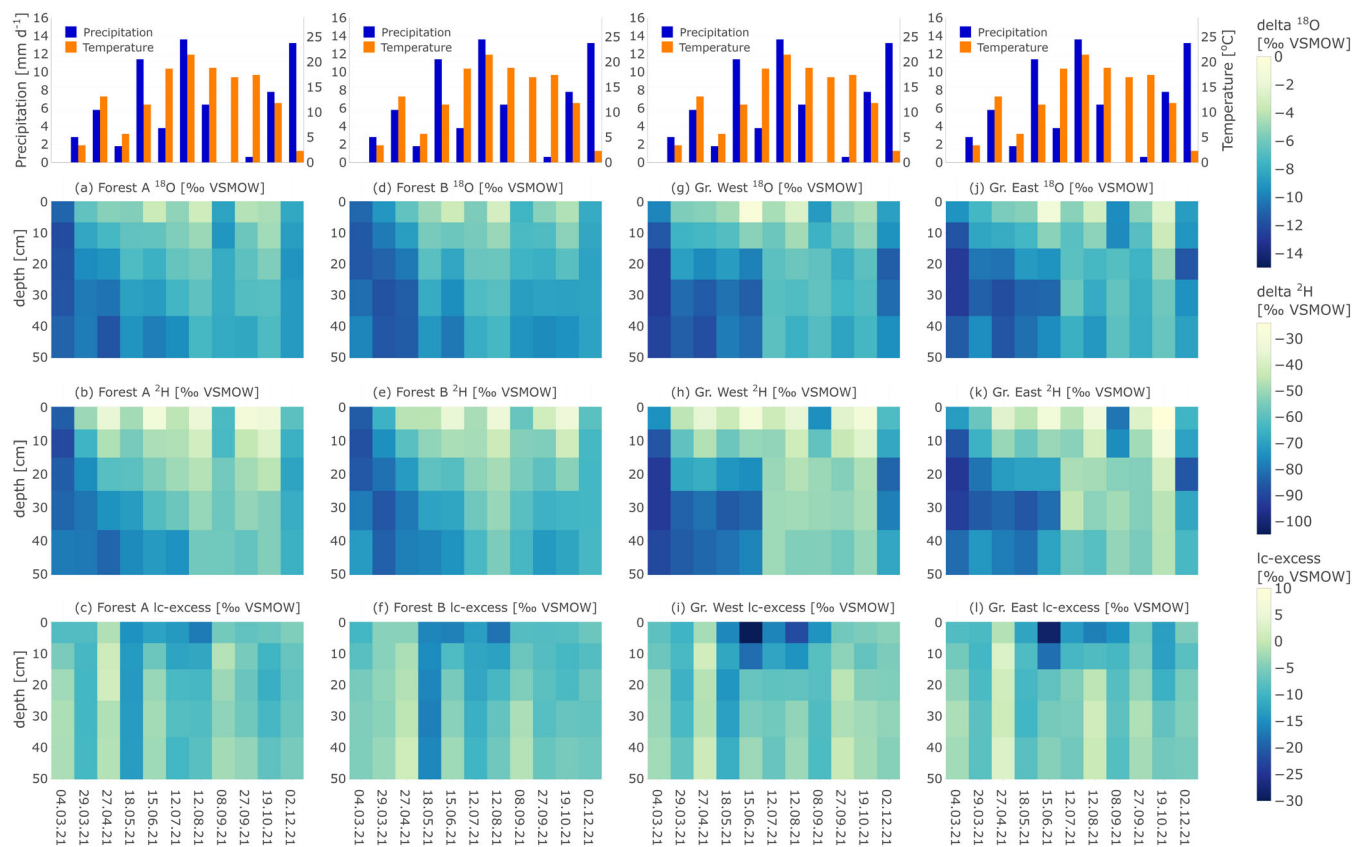


**FIGURE 5** Heat maps of bulk isotopes for *Forest A* (a–c), *Forest B* (d–f), *Grassland West* (g–i), and *East* (j–l). Top histograms show precipitation sum over the previous 7 days and air temperature on the sampling date

Soil water storage was highest at sites with conventional arable land use, followed by innovative arable land use (agroforestry) and grasslands, with forests being driest. Partly this reflects land use influences on ecohydrological partitioning (Gómez-Plaza et al., 2000; Hupet & Vanclooster, 2002; Schume et al., 2003), such as the higher evapotranspiration (due to interception) under the forest sites (see Smith et al., 2021). It also shows the strong influence of soil moisture and properties (see Geris et al., 2015; Grant et al., 2004). Sand soils, particularly under forest, were driest and less water retentive, while loams as more retentive soils, are the focal areas for agriculture. Previous investigations by Smith, Tetzlaff, Kleine, et al. (2020b) and Kleine et al. (2020) in DMC demonstrated similar dependencies between soil moisture dynamics, soil properties and land use at forest (drier sand soils) and grassland (wetter loam) plots.

Conventional arable sites had high soil moisture due to shallow rooting systems (down to ~60 cm) and ploughing (down to ~20 cm). At the agroforestry sites, there is a suggestion that the deeper soil layers were also affected by root water uptake (see Figures S2 and S3) due to deeper rooting systems of clover (40–210 cm). Shelter belt trees and other legumes have been shown to use more water compared to crops (Blessing et al., 2018). At the grassland and agricultural sites, the deepest soil layer showed less dynamics in VWC while the forest sites also had dynamic responses down to 1 m due to deep-rooting trees, extracting deeper water, and the higher soil permeability (see Everson et al., 2009; Kleine et al., 2020). The grassland and forest sites had

lower VWC compared to the agricultural sites, which is likely due to the different soil properties of the sites. Previously, forests were observed to have lower VWC compared to grassland sites due to higher interception and transpiration loss in forests (Douinot et al., 2019; Kleine et al., 2020; Zhang & Shanguan, 2016). Other studies by James et al. (2003) and Williams et al. (2012) found grassland to be drier and with higher variability compared to forest, which might be due to the studies only covering topsoil (10 and 30 cm) or forest sites with negligible groundwater input. At such locations, evaporative effects on grassland may become more influential than in a shaded forest with the deeper rooting systems and more distributed root water uptake across depth. Of course, the combination of many factors like topography, soil properties, and hydroclimatic conditions dictate soil water content VWC (see Neill et al., 2021; Zhu & Lin, 2011; Zucco et al., 2014). Nevertheless, in our study, the time dependent effects of dominant vegetation showed a clear influence on the patterns of ecohydrological partitioning of soil moisture variability, for example, forest soils tended to be drier compared to those under grassland.

## 4.2 | Effects of land use on soil water isotopic compositions

Perhaps a little surprisingly, all sites showed relatively similar isotopic compositions in dual isotope space indicating no substantial variability



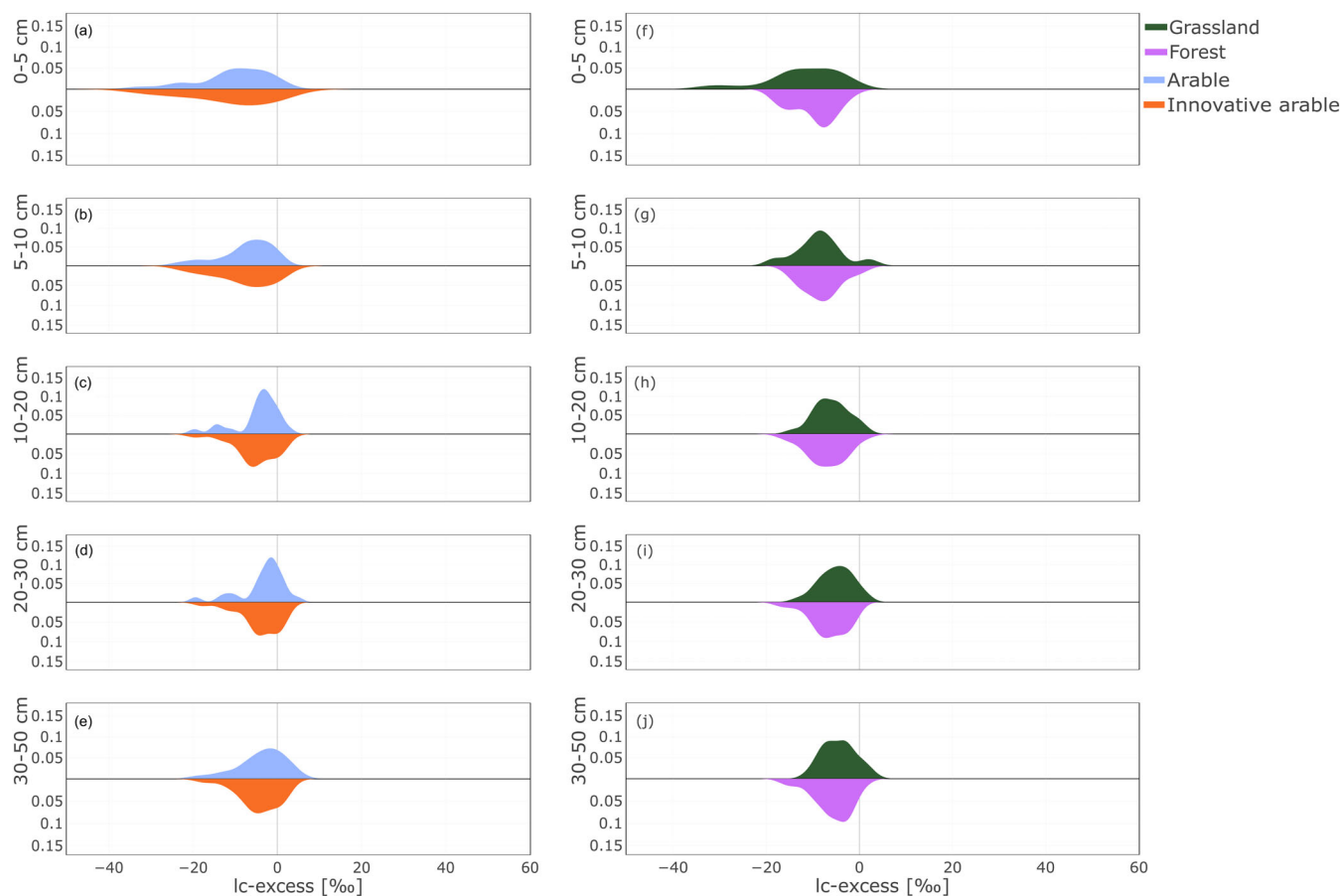


**FIGURE 6** Kernel density estimation of arable (*Crops* and *Legumes rotation* combined), innovative arable (*Pasture with shelter belt* and *Syntropic*), *Grassland* (*West* and *East* combined), and *Forest* (*A* and *B* combined) sites for  $lc\text{-excess}$  (a–j)

between the monitored land uses, particularly in terms of evaporative effects. Despite this, the more gradual variability of the forest site soil water composition in the heat maps indicates deviation from the other sites due to land use. For example, in the forest, its deeper rooting system combined with minor ground vegetation allowed the evaporative front to penetrate deeper into the soil profile (see Kleine et al., 2020; Oerter & Bowen, 2019) as roots at deeper depths also lead to drier condition in these layers. The already dry conditions of the forest soils resulting in proportionally more marked effects of evapotranspiration and no direct soil cover leads to direct interactions between soil and atmosphere (see Sprenger et al., 2017).

Conventional and innovative agricultural sites showed no substantial differences in isotopic composition. It is likely that the early stage of vegetation in the innovative sites (*Syntropic* was planted in 2019 and *Pasture* in 2021) is reflected in the observed similarity of these to conventional arable sites. The young trees or shrubs in their current life-stage likely compete for resources with the clover as similar effects were observed in other studies of agroforestry (see Everson et al., 2009; Sollen-Norrin et al., 2020). However, this will most likely change as soon as the trees develop progressively deeper rooting systems filling a different spatial niche as clover or crops (see Everson et al., 2009; Guo & Zhao, 2021).

To assess such influences and feedbacks as well as their timing (when exactly will the trees/shrubs be in a different niche as the clover/crops) long-term observations or repeats of surveys in a few years would be necessary (see Tetzlaff et al., 2017). Tracking soil water isotopes (as well as soil moisture) in long-term studies has key potential for showing how water partitioning changes over time and under climatic non-stationarity. In particular, the effects of evaporation on fractionation change as vegetation under new land uses develops, which will also change how precipitation mixes with resident soil water, as soil structure changes and rooting zones develop. Of course, given the resource intensive, destructive nature of the sampling, such monitoring would usually be infeasible as part of routine monitoring, but repeats surveys during growing seasons every 3–5 years could be highly informative.

### 4.3 | The role of land use on water partitioning

It is already well-established that the vegetation characteristics of different land uses affect water partitioning via canopy structure and foliage density, soil coverage, rooting structure, and creating new habitats for soil organisms that can in turn affect soil properties (see



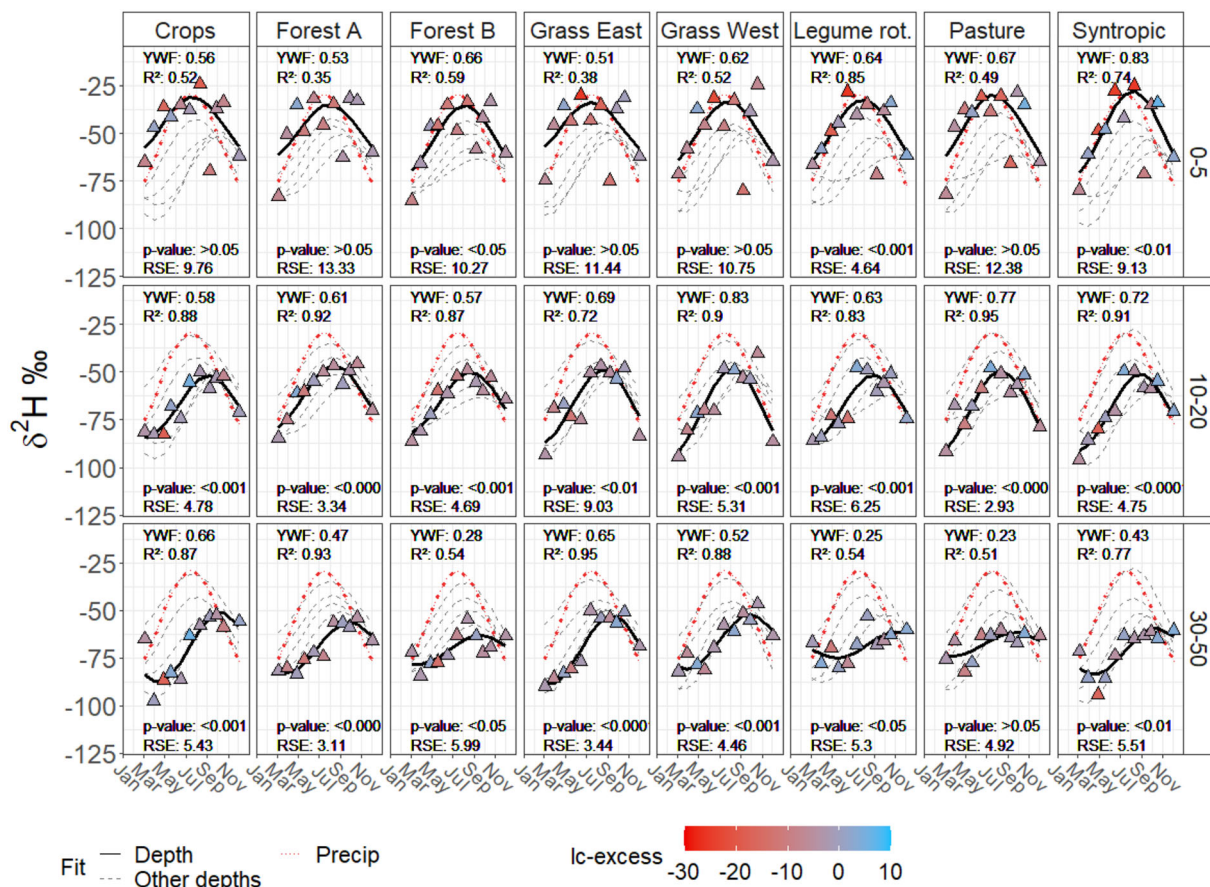


**FIGURE 7** Young water fraction for all sites and three of the depths. The fit of soil water  $\delta^2\text{H}$  of the according depth is shown as a black line. Additionally,  $\delta^2\text{H}$  fits of all other depths (also the ones not presented by a panel in the plot) are represented by a dotted grey line. Precipitation is shown as a dotted red line and l-excess amounts are shown by the triangle coloration. YWF,  $R^2$ , p-value, and RSE (residual sum of squares) values are given in the graphs as text

Douinot et al., 2019; Morazzo et al., 2022). Under the hydroclimatic conditions of 2021, which was relatively wet, and dominated by a large mid-summer storm event, we found that influence of land use on soil moisture storage was largely restricted to arable and innovative (agroforestry) crops being wetter than forests and, to a lesser extent, grasslands. Such differences would probably be accentuated under drier conditions, particularly droughts when heterogeneity in vegetation and soil properties become more dominant controls (see Kleine et al., 2020). The precipitation input of 2021 was comparable to the long-term annual mean, however, precipitation distribution over the year, especially during summer, was still insufficient to replenish high evapotranspirational losses. For example, even the large precipitation event in June was not able to refill the soil moisture deficits at all sites, particularly under forests. The precipitation patterns we observed in 2021 at the DMC fit findings of shifting precipitation events (more rain during winter and less in summer) as well as more extreme events (large precipitation events followed by prolonged droughts) due to climate change (Wunsch et al., 2022).

Further, we observed a strong correlation between PET and soil isotopes at the DMC as high atmospheric moisture demand resulted in evaporative fractionation of soil water. The response of soil water l-excess to evaporation demands resulted in a weak hysteresis

pattern as well as the YWF components of the soil water showing a time lag, which likely occurred due to mixing processes of the soil water with incoming precipitation (see Kleine et al., 2020; Sprenger et al., 2017). In general, the isotopic composition of arable sites and grassland were similar while the forest sites differed substantially from the other land use types. This is probably driven by both the different soil properties (poorer, sandier soils inhabit the forests) and the higher demand of water by forests compared to grassland or crops (see Douinot et al., 2019; Kleine et al., 2020). The similarity between grassland and arable sites is likely caused by the wet conditions produced by large precipitation events during summer interrupting the evaporative fractionation in summer. The innovative agroforestry sites were similar to conventional sites, most likely due to their early development stage. This shows that it is important to start water-sensitive approaches to land use management early, as land use changes may take years to decades before effects become apparent.

#### 4.4 | Wider implications

Our study showed the similarities and differences between grassland, arable and forest sites by utilizing stable water isotopes as tracers to

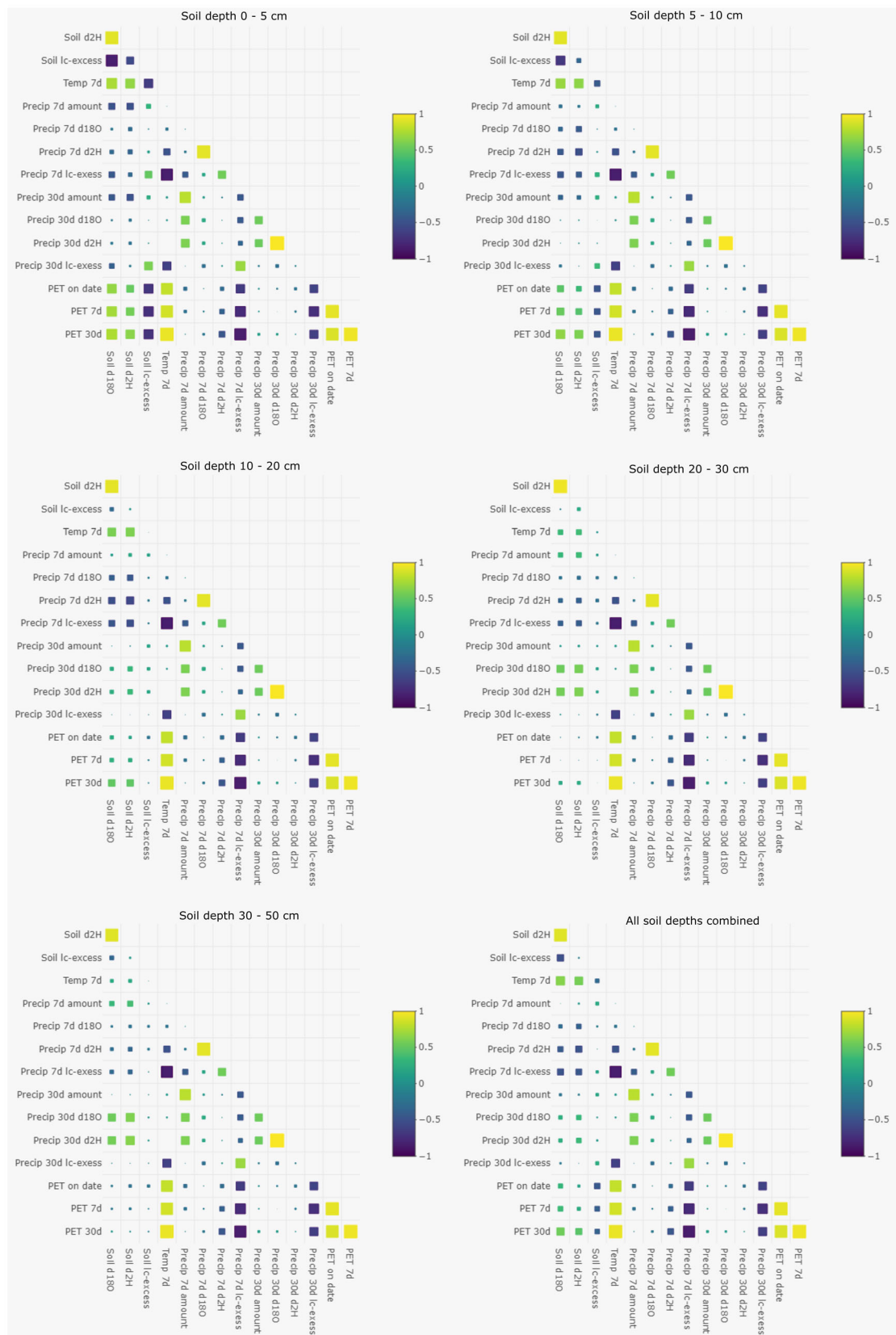


**FIGURE 8** Pearson correlation between PET on sampling date ('PET on date'), PET sum over 7 days ('PET<sub>7d</sub>'), PET sum over 30 days ('PET<sub>30d</sub>'), precipitation amount sum over 7 days ('Precipitation<sub>7d</sub>'), precipitation amount sum over 30 days ('Precipitation<sub>30d</sub>'), precipitation  $\delta^{18}\text{O}$  ('Precipitation<sub>7d</sub> 180'),  $\delta^2\text{H}$  ('Precipitation<sub>7d</sub> 2H'), and lc-excess ('Precipitation<sub>7d</sub> lc-excess') mean over 7 days, precipitation  $\delta^{18}\text{O}$  ('Precipitation<sub>30d</sub> 180'),  $\delta^2\text{H}$  ('Precipitation<sub>30d</sub> 2H'), and lc-excess ('Precipitation<sub>30d</sub> lc-excess') mean over 30 days, air temperature mean over 7 days ('Temperature<sub>7d</sub>'), soil  $\delta^{18}\text{O}$  ('Soil d180'), soil  $\delta^2\text{H}$  ('Soil d2H'), and soil lc-excess ('Soil lc'). The different plots show different depth intervals of 0–5, 5–10, 10–20, 20–30, 30–50 cm, and all depths combined

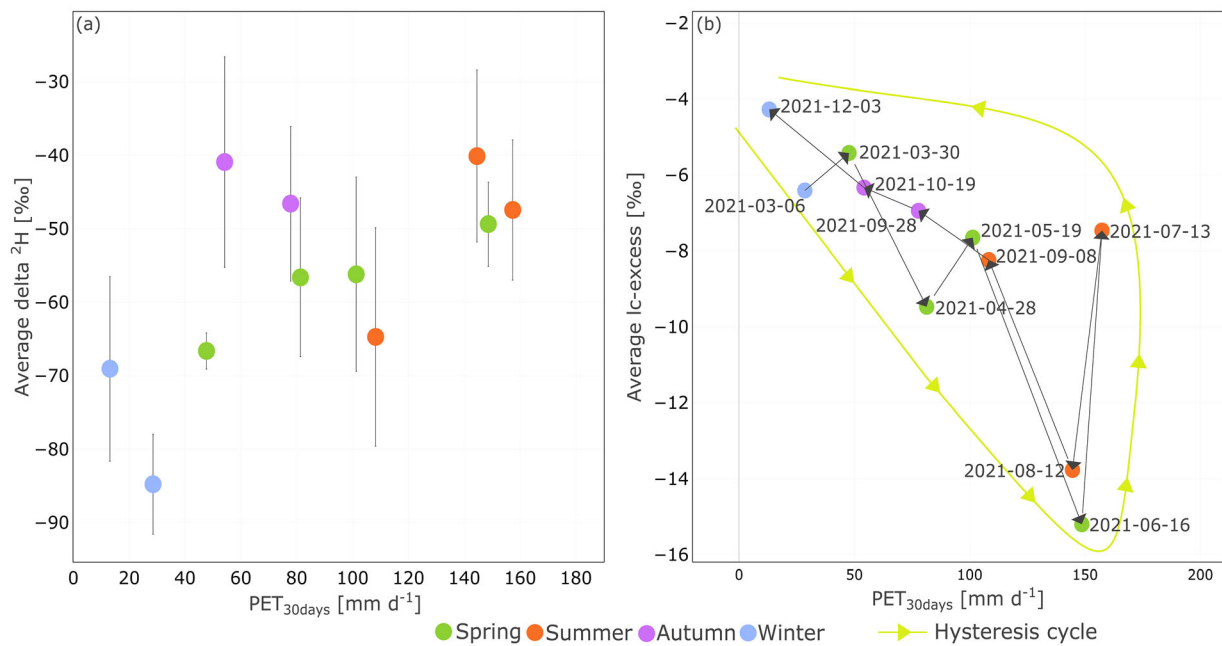


**FIGURE 9** Top 20 cm variability of soil  $\delta^2\text{H}$  (a) and lc-excess (b) as a function of the PET averaged over 30 days prior to sampling ( $\text{PET}_{30}$ ). The coloration of the data points represents the season of sampling. The standard deviation of the samples is indicated by the error bars in (a). The order of the sampling dates is represented by arrows in (b) with a theoretical hysteresis cycle. In both plots the grassland and forest sites were sampled at 1 day while the arable sites (including pasture and syntropic) were sampled the other day. All the soil results and  $\text{PET}_{30\text{days}}$  were aggregated to present only one data point for each sampling set (e.g., 2021-03-06 is the aggregated result of 2021-03-05 and 2021-03-06)

investigate blue and green water fluxes. Isotopic investigations like the one in our study have great potential to be incorporated in tracer-aided models to resolve and quantify the green water fluxes under different land use (Kuppel et al., 2018; Parnell et al., 2010). As dry summers are likely to become more common due to climate change, freely draining soil properties and non-irrigated agriculture pose challenges to sustainable land management in the DMC, and extensive areas in the lowlands of central Europe with similar characteristics. Resilience to withstand droughts and the increasing stress of prolonged water scarcity will be strongly dependent on land use. Therefore, understanding and quantifying water partitioning in systems like the DMC is especially important to manage soil moisture in the unsaturated zone and maintain societally important ecosystem services. As forests, grasslands and crops all depend on shallow soil water as well as refilling of groundwater storage, there has to be an informed assessment of the trade-off between ecosystem services like biomass production or groundwater recharge. The management of those ecosystems will be most sustainable if we understand the partitioning processes of blue and green water fluxes as well as their impacts.

This study revealed that forests are already potentially vulnerable landscapes of the DMC as they showed lowest soil water storage (compared to crops and grassland). Further, recently established innovative agricultural sites involving agroforestry still did not show significant changes in water partitioning compared to conventional arable sites. Agroforestry sites may create similarities to forests given potential for deeper rooting and increased canopy cover. Therefore, sustainable land use strategies might require more or earlier management

and decision making than expected. In addition, the effects of the land use change on ecohydrological partitioning in their extent and timing might deliver useful results for planning such land use strategies. Hence, we recommend further long-term investigations embedding plot scale studies in catchment scale monitoring of blue water fluxes within sustainable land use projects more fully. Further, we suggest that these long-term observations should include stable water isotopes as natural tracers of the water fluxes together with meteorological monitoring and model development.

## 5 | CONCLUSIONS

We investigated the effects of different land use on soil moisture dynamics and water partitioning via stable water isotopes comparing it to other environmental factors in a lowland headwater catchment (DMC) in NE Germany. At the scope of our study were four different land use types at eight plot sites with varies soil properties monitored over an entire growing period. In general, 2021 was a year with a relatively wet growing period with large mid-summer storm events resulting in similar soil water isotopic compositions for most of the sites. Differences in water partitioning due to vegetation cover will be likely stronger under drier conditions. The forest sites were influenced by highest interception and transpiration losses, resulting in lowest soil water storage and differing from the other sites in soil water isotopic composition. The innovative (agroforestry) sites were similar to conventional arable sites and grassland due to the early life-stage of the

trees. Topsoil water was younger, and with increasing depth, the soil water became older. Forests showed low fractions of young water (<2–3 months) especially in the deeper soil layers even though the lag times were low (46 days) indicating low young water input into the forest system due to high interception and transpiration loss. The other study sites showed higher YWFs and were affected by the large storm events in mid-summer into their deeper soil layers revealing their higher potential for groundwater recharge compared to the forest sites. These findings have increased our knowledge of land use induced impacts on water partitioning in lowland mixed land use catchments, but also underscore the need for repeated surveys of stable water isotopes in changing systems every 3–5 years. In conjunction with hydroclimate monitoring, such surveys will detect vegetation and land management induced changes supporting the value of tracer-based models to resolve and quantify green water fluxes. Further research efforts on water partitioning under various vegetation and land use types are needed to mitigate the effects of climate change on vulnerable landscapes and to develop water and land management adaptations for economic land use changes.

#### ACKNOWLEDGEMENTS

We acknowledge the BMBF (funding code 033W034A) which supported the stable isotope laboratory and the Open Access Publication Fund by IGB and the Leibniz Association's Open Access Publishing Fund. Funding for DT was also received through the Einstein Research Unit 'Climate and Water under Change' from the Einstein Foundation Berlin and Berlin University Alliance. Contributions from CS were supported by the Leverhulme Trust through the ISOLAND project (Grant No. RPG 2018 375). The authors are grateful to Hauke Dämpfung, and Jan Christopher who were involved in the setup and maintenance of the monitoring systems of the DMC. We also thank David Dubbert for stable water isotope analysis and Christian Marx for creating an R script processing soil stable water isotope data. We thank the colleagues from the Finck Foundation ([www.finck-stiftung.org](http://www.finck-stiftung.org)) for the trustful collaboration, for providing access to the study sites (with different, also regenerative, multifunctional land uses) and for supporting our study with their experiences of climate and soil effects during the transition to regenerative land use models. We are thankful for the technical support by the WLV (Wasser und Landschaftspflegeverband Untere Spree). Further, we thank Aaron Andrew Smith for discussing several statistical approaches, and Jan Christopher and Ralf Parsche for their help in soil sampling.

#### DATA AVAILABILITY STATEMENT

Research data are not shared.

#### ORCID

Jessica Landgraf  <https://orcid.org/0000-0003-3207-7515>

Dörthe Tetzlaff  <https://orcid.org/0000-0002-7183-8674>

Songjun Wu  <https://orcid.org/0000-0003-1758-5714>

Chris Soulsby  <https://orcid.org/0000-0001-6910-2118>

#### REFERENCES

- Allen, R. G., Pereira, L. S., Raes, D., & Smith, M. (1998). *FAO irrigation and drainage paper no. 56* (Vol. 56(97), p. e156). Food and Agriculture Organization of the United Nations.
- Balist, J., Malekmohammadi, B., Jafari, H. R., Nohegar, A., & Geneletti, D. (2022). Detecting land use and climate impacts on water yield ecosystem service in arid and semi-arid areas. A study in Sirvan River Basin-Iran. *Applied Water Science*, 12(1), 1–14. <https://doi.org/10.1007/s13201-021-01545-8>
- Beyer, M., Kühnhammer, K., & Dubbert, M. (2020). In situ measurements of soil and plant water isotopes: A review of approaches, practical considerations and a vision for the future. *Hydrology and Earth System Sciences*, 24(9), 4413–4440. <https://doi.org/10.5194/hess-24-4413-2020>
- Blessing, C. H., Mariette, A., Kaloki, P., & Bramley, H. (2018). Profligate and conservative: Water use strategies in grain legumes. *Journal of Experimental Botany*, 69(3), 349–369. <https://doi.org/10.1093/jxb/erx415>
- Brás, T. A., Seixas, J., Carvalhais, N., & Jägermeyr, J. (2021). Severity of drought and heatwave crop losses tripled over the last five decades in Europe. *Environmental Research Letters*, 16(6), 065012. <https://doi.org/10.1088/1748-9326/abf004>
- Burba, G. (2013). *Eddy covariance method for scientific, industrial, agricultural and regulatory applications: A field book on measuring ecosystem gas exchange and areal emission rates*. LI-COR Biosciences, ISBN 978-0-615-76827-4.
- Deutscher Wetterdienst. (2021). *DWD [data set]*. [https://opendata.dwd.de/climate\\_environment/CDC/observations\\_germany/climate/daily/more\\_precip/recent/](https://opendata.dwd.de/climate_environment/CDC/observations_germany/climate/daily/more_precip/recent/)
- Douinot, A., Tetzlaff, D., Maneta, M., Kuppel, S., Schulte-Bisping, H., & Soulsby, C. (2019). Ecohydrological modelling with Ech2O-iso to quantify forest and grassland effects on water partitioning and flux ages. *Hydrological Processes*, 33(16), 2174–2191. <https://doi.org/10.1002/hyp.13480>
- Everson, C. S., Everson, T. M., & Van Niekerk, W. (2009). Soil water competition in a temperate hedgerow agroforestry system in South Africa. *Agroforestry Systems*, 75(3), 211–221. <https://doi.org/10.1007/s10457-008-9174-x>
- Falkenmark, M., & Rockström, J. (2006). The new blue and green water paradigm: Breaking new ground for water resources planning and management. *Journal of Water Resources Planning and Management*, 132(3), 129–132. [https://doi.org/10.1061/\(ASCE\)0733-9496\(2006\)132:3\(129\)](https://doi.org/10.1061/(ASCE)0733-9496(2006)132:3(129))
- Foley, J. A., DeFries, R., Asner, G. P., Barford, C., Bonan, G., Carpenter, S. R., Chapin, S. F., Coe, M. T., Daily, G. C., Gibbs, H. K., Helkowski, J. H., Holloway, T., Howard, E. A., Kucharik, J., Monfreda, C., Patz, J. A., Prentice, I. C., Ramankutty, N., & Snyder, P. K. (2005). Global consequences of land use. *Science*, 309(5734), 570–574. <https://doi.org/10.1126/science.1111772>
- Friesen, J., & Van Stan, J. T. (2019). Early European observations of precipitation partitioning by vegetation: A synthesis and evaluation of 19th century findings. *Geosciences*, 9(10), 423. <https://doi.org/10.3390/geosciences9100423>
- Gelbrecht, J., Fait, M., Dittrich, M., & Steinberg, C. (1998). Use of GC and equilibrium calculations of CO<sub>2</sub> saturation index to indicate whether freshwater bodies in north-eastern Germany are net sources or sinks for atmospheric CO<sub>2</sub>. *Fresenius' Journal of Analytical Chemistry*, 361(1), 47–53. <https://doi.org/10.1007/s002160050832>
- Gelbrecht, J., Lengsfeld, H., Pöthig, R., & Opitz, D. (2005). Temporal and spatial variation of phosphorus input, retention and loss in a small catchment of NE Germany. *Journal of Hydrology*, 304(1–4), 151–165. <https://doi.org/10.1016/j.jhydrol.2004.07.028>
- Geris, J., Tetzlaff, D., McDonnell, J., & Soulsby, C. (2015). The relative role of soil type and tree cover on water storage and transmission in northern headwater catchments. *Hydrological Processes*, 29(7), 1844–1860. <https://doi.org/10.1002/hyp.10289>



- GeoBasis-DE/BKG. (2018). *Federal agency for cartography and geodesy*. <https://gdz.bkg.bund.de/index.php/default/corine-land-cover-5-stand-2018-cls5-2018.html>
- Goldsmith, G. R., Muñoz-Villers, L. E., Holwerda, F., McDonnell, J. J., Asbjørnsen, H., & Dawson, T. E. (2012). Stable isotopes reveal linkages among ecohydrological processes in a seasonally dry tropical montane cloud forest. *Ecohydrology*, 5(6), 779–790. <https://doi.org/10.1002/eco.268>
- Gómez-Plaza, A., Alvarez-Rogel, J., Albaladejo, J., & Castillo, V. M. (2000). Spatial patterns and temporal stability of soil moisture across a range of scales in a semi-arid environment. *Hydrological Processes*, 14(7), 1261–1277. [https://doi.org/10.1002/\(SICI\)1099-1085\(200005\)14:7<1261::AID-HYP40>3.0.CO;2-D](https://doi.org/10.1002/(SICI)1099-1085(200005)14:7<1261::AID-HYP40>3.0.CO;2-D)
- Grant, L., Seyfried, M., & McNamara, J. (2004). Spatial variation and temporal stability of soil water in a snow-dominated, mountain catchment. *Hydrological Processes*, 18(18), 3493–3511. <https://doi.org/10.1002/hyp.5798>
- Guo, H., & Zhao, Y. (2021). Using isotopic labeling to investigate root water uptake in an alley cropping system within Taklimakan Desert Oasis, China. *Agroforestry Systems*, 95(5), 907–918. <https://doi.org/10.1007/s10457-020-00527-0>
- Hänsel, S., Hoy, A., Brendel, C., & Maugeri, M. (2022). Record summers in Europe: Variations in drought and heavy precipitation during 1901–2018. *International Journal of Climatology*, 42(12), 6235–6257. <https://doi.org/10.1002/joc.7587>
- Hopp, L., Harman, C., Desilets, S. L., Graham, C. B., McDonnell, J. J., & Troch, P. A. (2009). Hillslope hydrology under glass: Confronting fundamental questions of soil-water-biota co-evolution at Biosphere 2. *Hydrology and Earth System Sciences*, 13(11), 2105–2118. <https://doi.org/10.5194/hess-13-2105-2009>
- Hughes, C. E., & Crawford, J. (2012). A new precipitation weighted method for determining the meteoric water line for hydrological applications demonstrated using Australian and global GNIP data. *Journal of Hydrology*, 464–465, 344–351. <https://doi.org/10.1016/j.jhydrol.2012.07.029>
- Hupet, F., & Vanclooster, M. (2002). Intra-seasonal dynamics of soil moisture variability within a small agricultural maize cropped field. *Journal of Hydrology*, 261(1–4), 86–101. [https://doi.org/10.1016/S0022-1694\(02\)00016-1](https://doi.org/10.1016/S0022-1694(02)00016-1)
- IAEA/GNIP. (2014). *Precipitation sampling guide V2.02, September 2014*.
- Jacob, D., Petersen, J., Eggert, B., Alias, A., Christensen, O. B., Bouwer, L. M., Braun, A., Colette, A., Déqué, M., Georgievski, G., Georgopoulou, E., Gobiet, A., Menut, L., Nikulin, G., Haensler, A., Hempelmann, N., Jones, C., Keuler, K., Kovats, S., & Yiou, P. (2014). EURO-CORDEX: New high-resolution climate change projections for European impact research. *Regional Environmental Change*, 14(2), 563–578. <https://doi.org/10.1007/s10113-013-0499-2>
- James, S. E., Pärtel, M., Wilson, S. D., & Peltzer, D. A. (2003). Temporal heterogeneity of soil moisture in grassland and forest. *Journal of Ecology*, 91(2), 234–239. <https://doi.org/10.1046/j.1365-2745.2003.00758.x>
- Kirchner, J. W. (2016a). Aggregation in environmental systems – Part 2: Catchment mean transit times and young water fractions under hydrologic nonstationarity. *Hydrology and Earth System Sciences*, 20(1), 299–328. <https://doi.org/10.5194/hess-20-299-2016>
- Kirchner, J. W. (2016b). Aggregation in environmental systems – Part 1: Seasonal tracer cycles quantify young water fractions, but not mean transit times, in spatially heterogeneous catchments. *Hydrology and Earth System Sciences*, 20(1), 279–297. <https://doi.org/10.5194/hess-20-279-2016>
- Kleine, L., Tetzlaff, D., Smith, A., Dubbert, M., & Soulsby, C. (2021). Modelling ecohydrological feedbacks in forest and grassland plots under a prolonged drought anomaly in central Europe 2018–2020. *Hydrological Processes*, 35(8), e14325. <https://doi.org/10.1002/hyp.14325>
- Kleine, L., Tetzlaff, D., Smith, A., Goldammer, T., & Soulsby, C. (2021). Using isotopes to understand landscape-scale connectivity in a groundwater-dominated, lowland catchment under drought conditions. *Hydrological Processes*, 35(5), e14197. <https://doi.org/10.1002/hyp.14197>
- Kleine, L., Tetzlaff, D., Smith, A., Wang, H., & Soulsby, C. (2020). Using water stable isotopes to understand evaporation, moisture stress, and re-wetting in catchment forest and grassland soils of the summer drought of 2018. *Hydrology and Earth System Sciences*, 24(7), 3737–3752. <https://doi.org/10.5194/hess-24-3737-2020>
- Kühnhammer, K., Kübert, A., Brüggemann, N., Deseano Diaz, P., van Dusschoten, D., Javaux, M., Merz, S., Vereecken, H., Dubbert, M., & Rothfuss, Y. (2020). Investigating the root plasticity response of *Centaurea jacea* to soil water availability changes from isotopic analysis. *New Phytologist*, 226(1), 98–110. <https://doi.org/10.5194/hess-24-4413-2020>
- Kuppel, S., Tetzlaff, D., Maneta, M. P., & Soulsby, C. (2018). Ech2O-iso 1.0: Water isotopes and age tracking in a process-based, distributed ecohydrological model. *Geoscientific Model Development*, 11(7), 3045–3069. <https://doi.org/10.5194/gmd-11-3045-2018>
- Laganière, J., Augusto, L., Hatten, J. A., & Spielvogel, S. (2022). Editorial: Vegetation effects on soil organic matter in forested ecosystems. *Forests and Global Change*, 4, 82870. <https://doi.org/10.3389/ffgc.2021.828701>
- Landgraf, J., Tetzlaff, D., Dubbert, M., Dubbert, D., Smith, A., & Soulsby, C. (2022). Xylem water in riparian willow trees (*Salix alba*) reveals shallow sources of root water uptake by in situ monitoring of stable water isotopes. *Hydrology and Earth System Sciences*, 26(8), 2073–2092. <https://doi.org/10.5194/hess-26-2073-2022>
- Landwehr, J. M. M., & Coplen, T. B. (2006). Line-conditioned excess: A new method for characterizing stable hydrogen and oxygen isotope ratios in hydrologic systems. In *International Conference on Isotopes in Environmental Studies* (pp. 132–135). IAEA.
- Monteith, J. L. (1965). Evaporation and environment. In *Symposia of the society for experimental biology* (Vol. 19, pp. 205–234). Cambridge University Press (CUP).
- Marx, C., Tetzlaff, D., Hinkelmann, R., & Soulsby, C. (2022). Seasonal variations in soil-plant interactions in contrasting urban green spaces: Insights from water stable isotopes. *Journal of Hydrology*, 612, 127998. <https://doi.org/10.1016/j.jhydrol.2022.127998>
- Maurice, G. D. (2013). *College on soil physics-30th anniversary (1983-2013)*.
- Moravec, V., Markonis, Y., Rakovec, O., Svoboda, M., Trnka, M., Kumar, R., & Hanel, M. (2021). Europe under multi-year droughts: How severe was the 2014–2018 drought period? *Environmental Research Letters*, 16(3), 034062. <https://doi.org/10.1088/1748-9326/abe828>
- Morazzo, G., Riestra, D. R., Leizica, E., Álvarez, L., & Noellemeyer, E. (2022). Afforestation with different tree species causes a divergent evolution of soil profiles and properties. *Frontiers in Forests and Global Change*, 4, 685827. <https://doi.org/10.3389/ffgc.2021.685827>
- Msigwa, A., Komakech, H. C., Salvatore, E., Seyoum, S., Mul, M. L., & van Griensven, A. (2021). Comparison of blue and green water fluxes for different land use classes in a semi-arid cultivated catchment using remote sensing. *Journal of Hydrology: Regional Studies*, 36, 100860. <https://doi.org/10.1016/j.ejrh.2021.100860>
- Neill, A. J., Birkel, C., Maneta, M. P., Tetzlaff, D., & Soulsby, C. (2021). Structural changes to forests during regeneration affect water flux partitioning, water ages and hydrological connectivity: Insights from tracer-aided ecohydrological modelling. *Hydrology and Earth System Sciences*, 25(9), 4861–4886. <https://doi.org/10.5194/hess-25-4861-2021>
- Oerter, E. J., & Bowen, G. J. (2019). Spatio-temporal heterogeneity in soil water stable isotopic composition and its ecohydrologic implications in semiarid ecosystems. *Hydrological Processes*, 33(12), 1724–1738. <https://doi.org/10.1002/hyp.13434>
- Orth, R., & Destouni, G. (2018). Drought reduces blue-water fluxes more strongly than green-water fluxes in Europe. *Nature Communications*, 9(1), 1–8. <https://doi.org/10.1038/s41467-018-06013-7>

- Parnell, A. C., Inger, R., Bearhop, S., & Jackson, A. L. (2010). Source partitioning using stable isotopes: Coping with too much variation. *PLoS One*, 5(3), e9672. <https://doi.org/10.1371/journal.pone.0009672>
- Penman, H. L. (1948). Natural evaporation from open water, bare soil and grass. *Proceedings of the Royal Society of London, Series A: Mathematical and Physical Sciences*, 193(1032), 120–145.
- Rothfuss, Y., Biron, P., Braud, I., Canale, L., Durand, J. L., Gaudet, J. P., Richard, P., Vauclin, M., & Bariac, T. (2010). Partitioning evapotranspiration fluxes into soil evaporation and plant transpiration using water stable isotopes under controlled conditions. *Hydrological Processes*, 24(22), 3177–3194. <https://doi.org/10.1002/hyp.7743>
- Rothfuss, Y., Vereecken, H., & Brüggemann, N. (2013). Monitoring water stable isotopic composition in soils using gas-permeable tubing and infrared laser absorption spectroscopy. *Water Resources Research*, 49(6), 3747–3755. <https://doi.org/10.1002/wrcr.20311>
- Schume, H., Jost, G., & Katzensteiner, K. (2003). Spatio-temporal analysis of the soil water content in a mixed Norway spruce (*Picea abies* (L.) Karst.)–European beech (*Fagus sylvatica* L.) stand. *Geoderma*, 112(3–4), 273–287. [https://doi.org/10.1016/S0016-7061\(02\)00311-7](https://doi.org/10.1016/S0016-7061(02)00311-7)
- Senf, C., & Seidl, R. (2021). Persistent impacts of the 2018 drought on forest disturbance regimes in Europe. *Biogeosciences*, 18(18), 5223–5230. <https://doi.org/10.5194/bg-18-5223-2021>
- Smith, A., Tetzlaff, D., Gelbrecht, J., Kleine, L., & Soulsby, C. (2020). Riparian wetland rehabilitation and beaver re-colonization impacts on hydrological processes and water quality in a lowland agricultural catchment. *Science of the Total Environment*, 699, 134302. <https://doi.org/10.1016/j.scitotenv.2019.134302>
- Smith, A., Tetzlaff, D., Kleine, L., Maneta, M., & Soulsby, C. (2021). Quantifying the effects of land use and model scale on water partitioning and water ages using tracer-aided ecohydrological models. *Hydrology and Earth System Sciences*, 25(4), 2239–2259. <https://doi.org/10.5194/hess-25-2239-2021>
- Smith, A., Tetzlaff, D., Kleine, L., Maneta, M. P., & Soulsby, C. (2020b). Isotope-aided modelling of ecohydrologic fluxes and water ages under mixed land use in Central Europe: The 2018 drought and its recovery. *Hydrological Processes*, 34(16), 3406–3425. <https://doi.org/10.1002/hyp.13838>
- Smith, A. A., Tetzlaff, D., Kleine, L., Maneta, M., & Soulsby, C. (2020a). Upscaling land use effects on water partitioning and water ages using tracer-aided ecohydrological models. *Hydrology and Earth System Sciences*. <https://doi.org/10.5194/hess-2020-539>
- Sollen-Norrlin, M., Ghaley, B. B., & Rintoul, N. L. J. (2020). Agroforestry benefits and challenges for adoption in Europe and beyond. *Sustainability*, 12(17), 7001. <https://doi.org/10.3390/su12177001>
- Soulsby, C., Piegat, K., Seibert, J., & Tetzlaff, D. (2011). Catchment-scale estimates of flow path partitioning and water storage based on transit time and runoff modelling. *Hydrological Processes*, 25(25), 3960–3976. <https://doi.org/10.1002/hyp.8324>
- Sprenger, M., Tetzlaff, D., & Soulsby, C. (2017). Soil water stable isotopes reveal evaporation dynamics at the soil–plant–atmosphere interface of the critical zone. *Hydrology and Earth System Sciences*, 21(7), 3839–3858. <https://doi.org/10.5194/hess-21-3839-2017>
- Süßel, F., & Brüggemann, W. (2021). Tree water relations of mature oaks in southwest Germany under extreme drought stress in summer 2018. *Plant Stress*, 1, 100010. <https://doi.org/10.1016/j.stress.2021.100010>
- Tetzlaff, D., Buttle, J., Carey, S. K., Van Huijgevoort, M. H., Laudon, H., McNamara, J. P., Mitchell, C. P. J., Spence, C., Gabor, R. S., & Soulsby, C. (2015). A preliminary assessment of water partitioning and ecohydrological coupling in northern headwaters using stable isotopes and conceptual runoff models. *Hydrological Processes*, 29(25), 5153–5173. <https://doi.org/10.1002/hyp.10515>
- Tetzlaff, D., Carey, S. K., McNamara, J. P., Laudon, H., & Soulsby, C. (2017). The essential value of long-term experimental data for hydrology and water management. *Water Resources Research*, 53(4), 2598–2604. <https://doi.org/10.1002/2017WR020838>
- Thompson, S. E., Harman, C. J., Heine, P., & Katul, G. G. (2010). Vegetation-infiltration relationships across climatic and soil type gradients. *Journal of Geophysical Research: Biogeosciences*, 115(G2), 1–12. <https://doi.org/10.1029/2009JG001134>
- Volkman, T. H., & Weiler, M. (2014). Continual in situ monitoring of pore water stable isotopes in the subsurface. *Hydrology and Earth System Sciences*, 18(5), 1819–1833. <https://doi.org/10.5194/hess-18-1819-2014>
- von Freyberg, J., Allen, S. T., Seeger, S., Weiler, M., & Kirchner, J. W. (2018). Sensitivity of young water fractions to hydro-climatic forcing and landscape properties across 22 Swiss catchments. *Hydrology and Earth System Sciences*, 22(7), 3841–3861. <https://doi.org/10.5194/hess-22-3841-2018>
- Wassenaar, L. I., Hendry, M. J., Chostner, V. L., & Lis, G. P. (2008). High resolution pore water  $\delta^2\text{H}$  and  $\delta^{18}\text{O}$  measurements by  $\text{H}_2\text{O}$  (liquid)– $\text{H}_2\text{O}$  (vapor) equilibration laser spectroscopy. *Environmental Science & Technology*, 42(24), 9262–9267. <https://doi.org/10.1021/es802065s>
- Williams, C. A., Reichstein, M., Buchmann, N., Baldocchi, D., Beer, C., Schwalm, C., Wohlfahrt, G., Hasler, N., Bernhofer, C., Foken, T., Papale, D., Schymanski, S., & Schaefer, K. (2012). Climate and vegetation controls on the surface water balance: Synthesis of evapotranspiration measured across a global network of flux towers. *Water Resources Research*, 48(6), 1–13. <https://doi.org/10.1029/2011WR011586>
- Wunsch, A., Liesch, T., & Broda, S. (2022). Deep learning shows declining groundwater levels in Germany until 2100 due to climate change. *Nature Communications*, 13(1), 1–13. <https://doi.org/10.1038/s41467-022-28770-2>
- Zhang, Y. W., & Shangguan, Z. P. (2016). The change of soil water storage in three land use types after 10 years on the Loess Plateau. *Catena*, 147, 87–95. <https://doi.org/10.1016/j.catena.2016.06.036>
- Zhu, Q., & Lin, H. (2011). Influences of soil, terrain, and crop growth on soil moisture variation from transect to farm scales. *Geoderma*, 163(1–2), 45–54. <https://doi.org/10.1016/j.geoderma.2011.03.015>
- Ziche, D., Riek, W., Russ, A., Hentschel, R., & Martin, J. (2021). Water budgets of managed forests in northeast Germany under climate change—Results from a model study on forest monitoring sites. *Applied Sciences*, 11(5), 2403. <https://doi.org/10.3390/app11052403>
- Zucco, G., Brocca, L., Moramarco, T., & Morbidelli, R. (2014). Influence of land use on soil moisture spatial–temporal variability and monitoring. *Journal of Hydrology*, 516, 193–199. <https://doi.org/10.1016/j.jhydrol.2014.01.043>

## SUPPORTING INFORMATION

Additional supporting information can be found online in the Supporting Information section at the end of this article.

**How to cite this article:** Landgraf, J., Tetzlaff, D., Wu, S., Freymüller, J., & Soulsby, C. (2022). Using stable water isotopes to understand ecohydrological partitioning under contrasting land uses in a drought-sensitive rural, lowland catchment. *Hydrological Processes*, 36(12), e14779. <https://doi.org/10.1002/hyp.14779>